

Hybrid Feedback for Three-dimensional Convex Obstacle Avoidance (Extended version)

Mayur Sawant, Ilia Polushin and Abdelhamid Tayebi

Abstract—We propose a hybrid feedback control scheme for the autonomous robot navigation problem in three-dimensional environments with arbitrarily-shaped convex obstacles. The proposed hybrid control strategy, which consists in switching between the *move-to-target* mode and the *obstacle-avoidance* mode, guarantees global asymptotic stability of the target location in the obstacle-free workspace. We also provide a procedure for the implementation of the proposed hybrid controller in *a priori* unknown environments and validate its effectiveness through simulation results.

I. INTRODUCTION

Safe autonomous robot navigation consists in steering a robot to a target location while avoiding obstacles. One common method is the Navigation Function (NF) approach [1], where a combination of attractive and repulsive vector fields, with a properly tuned parameter, guarantees safe, almost¹ global convergence of the robot to the target location in sphere worlds. For general convex and star-shaped obstacles, diffeomorphic mappings [1], [2] allow the use of the NF approach but require complete knowledge of the environment. In [3], the NF method has been extended to convex obstacles that satisfy certain curvature properties, and are not too flat and not too close to the target. The work in [4] removes this flatness limitation, in environments with ellipsoidal obstacles, by using the Hessian to locally transform areas near obstacles into spherical regions. However, similar to [3], it is assumed that the entire shape of the obstacle is known when the robot visits its neighborhood.

In [5]–[7], the authors combine control Lyapunov functions (CLF) and control barrier functions (CBF) to design feedback laws that ensure safe convergence to a target location. The authors in [6] introduced a CBF-based method for multi-robot navigation in two-dimensional environments with circular obstacles. A comparative analysis between the APF and CBF approaches can be found in [7]. As shown in [8] and [9], CLF-CBF methods, like the NF approach, suffer from the undesired equilibria problem and guarantee, at best, almost global asymptotic stability in sphere worlds.

In [10], a feedback controller based on Nagumo’s theorem [11, Theorem 4.7] was proposed, guaranteeing safe, almost global convergence to the target location in *a priori* unknown environments with strongly convex obstacles. The work in [12] introduced a reactive navigation approach using separating hyperplanes for robots in environments with unknown, sufficiently separated, strongly convex obstacles.

However, the approaches discussed above provide, at best, almost global convergence guarantees due to the undesired equilibria that are generated when using continuous time-invariant vector fields [13]. This can be resolved by introducing discontinuities in the control, as shown in [14]–[17].

In [14], a discontinuous feedback law was developed for robot navigation in partially known two-dimensional environments, guiding the robot with the navigation function gradient near known obstacles and boundary-following near unknown ones. In [15], the authors proposed a discontinuous feedback controller for autonomous navigation of nonholonomic robots in two-dimensional environments with non-convex obstacles, imposing restrictions on the curvatures of obstacles’ boundaries and the inter-obstacle arrangements. In [16], the authors proposed a hybrid control law to globally asymptotically stabilize a class of linear systems with drift while avoiding neighborhoods of unsafe isolated points. In [17], hybrid control techniques were employed to achieve global stabilization of target locations in n -dimensional environments with sufficiently separated ellipsoidal obstacles.

In our earlier work [18], [19], we proposed a hybrid feedback control strategy for robot navigation in two-dimensional environments with convex and non-convex obstacles. In this paper, we extend this approach to ensure autonomous robot navigation in unknown 3-dimensional environments with arbitrarily-shaped convex obstacles, including those with non-smooth boundaries. Our solution guarantees safe, global asymptotic convergence of the robot to the target location, unlike the methods in [4], [10], [12], which guarantee, at best, almost global asymptotic convergence. The approach in [17] applies to environments with ellipsoidal obstacles, the work in [10], [12] is limited to strongly convex obstacles, and in [14], [15] the obstacles are required to have smooth boundaries. In contrast, the proposed hybrid feedback controller works for arbitrarily-shaped convex obstacles with no restrictions on inter-obstacle arrangement, except for a mild separation condition. We also propose a sensor-based version of our approach for autonomous navigation in *a priori* unknown 3-dimensional environments with arbitrarily-shaped convex obstacles.

This work was supported by the National Sciences and Engineering Research Council of Canada (NSERC), under the grants RGPIN-2020-06270, RGPIN-2020-0644 and RGPIN-2020-04759.

M. Sawant and A. Tayebi are with the Department of Electrical and Computer Engineering, Lakehead University, Thunder Bay, ON P7B 5E1, Canada. (e-mail: msawant, atayebi@lakeheadu.ca). I. Polushin is with the Department of Electrical and Computer Engineering, Western University, London, ON N6A 3K7, Canada. (e-mail: ipolushi@uwo.ca).

¹Almost global convergence refers to convergence from all initial locations except a set of zero Lebesgue measure.

II. NOTATIONS AND PRELIMINARIES

A. Notations

The sets of real and natural numbers are denoted by \mathbb{R} and \mathbb{N} , respectively. We identify vectors using bold lowercase letters. The Euclidean norm of a vector $\mathbf{p} \in \mathbb{R}^n$ is denoted by $\|\mathbf{p}\|$, and an Euclidean ball of radius $r \geq 0$ centered at \mathbf{p} is represented by $\mathcal{B}_r(\mathbf{p}) = \{\mathbf{q} \in \mathbb{R}^n \mid \|\mathbf{q} - \mathbf{p}\| \leq r\}$. The set of n -dimensional unit vectors is given by $\mathbb{S}^{n-1} = \{\mathbf{p} \in \mathbb{R}^n \mid \|\mathbf{p}\| = 1\}$. The identity matrix of order n is denoted by \mathbf{I}_n . The three-dimensional *Special Orthogonal group* is defined by $SO(3) := \{\mathbf{R} \in \mathbb{R}^{3 \times 3} : \mathbf{R}^\top \mathbf{R} = \mathbf{I}_3, \det(\mathbf{R}) = 1\}$. For a given vector $\mathbf{x} := [x_1, x_2, x_3]^\top \in \mathbb{R}^3$, we define \mathbf{x}^\times as the skew-symmetric matrix, which is given by

$$\mathbf{x}^\times = \begin{bmatrix} 0 & -x_3 & x_2 \\ x_3 & 0 & -x_1 \\ -x_2 & x_1 & 0 \end{bmatrix}. \quad (1)$$

For two sets $\mathcal{A}, \mathcal{B} \subset \mathbb{R}^n$, the relative complement of \mathcal{B} with respect to \mathcal{A} is denoted by $\mathcal{A} \setminus \mathcal{B} = \{\mathbf{a} \in \mathcal{A} \mid \mathbf{a} \notin \mathcal{B}\}$. The symbols $\partial\mathcal{A}$, \mathcal{A}° , \mathcal{A}^c and $\bar{\mathcal{A}}$ represent the boundary, interior, complement and the closure of the set \mathcal{A} , respectively, where $\partial\mathcal{A} = \bar{\mathcal{A}} \setminus \mathcal{A}^\circ$. The cardinality of a set \mathcal{A} is denoted by $\text{card}(\mathcal{A})$. The Minkowski sum of the sets \mathcal{A} and \mathcal{B} is denoted by $\mathcal{A} \oplus \mathcal{B} = \{\mathbf{a} + \mathbf{b} \mid \mathbf{a} \in \mathcal{A}, \mathbf{b} \in \mathcal{B}\}$. The dilated version of a set $\mathcal{A} \subset \mathbb{R}^n$ with $r \geq 0$ is represented by $\mathcal{D}_r(\mathcal{A}) = \mathcal{A} \oplus \mathcal{B}_r(\mathbf{0})$. The r -neighborhood of a set \mathcal{A} is denoted by $\mathcal{N}_r(\mathcal{A}) = \mathcal{D}_r(\mathcal{A}) \setminus \mathcal{A}^\circ$ where r is a strictly positive scalar.

B. Projection on a set

Given a closed set $\mathcal{A} \subset \mathbb{R}^n$ and a point $\mathbf{x} \in \mathbb{R}^n$, the Euclidean distance of \mathbf{x} from the set \mathcal{A} is evaluated as

$$d(\mathbf{x}, \mathcal{A}) = \min_{\mathbf{q} \in \mathcal{A}} \|\mathbf{x} - \mathbf{q}\|. \quad (2)$$

The set $\mathcal{PJ}(\mathbf{x}, \mathcal{A}) \subset \mathcal{A}$, which is defined as

$$\mathcal{PJ}(\mathbf{x}, \mathcal{A}) = \{\mathbf{q} \in \mathcal{A} \mid \|\mathbf{x} - \mathbf{q}\| = d(\mathbf{x}, \mathcal{A})\}, \quad (3)$$

is the set of points in \mathcal{A} that are at the distance of $d(\mathbf{x}, \mathcal{A})$ from \mathbf{x} . If $\text{card}(\mathcal{PJ}(\mathbf{x}, \mathcal{A}))$ is one, then the element of the set $\mathcal{PJ}(\mathbf{x}, \mathcal{A})$ is denoted by $\Pi(\mathbf{x}, \mathcal{A})$.

C. Geometric subsets of \mathbb{R}^n

1) *Line*: The line passing through two points $\mathbf{p} \in \mathbb{R}^n$ and $\mathbf{q} \in \mathbb{R}^n \setminus \{\mathbf{p}\}$ is given by

$$\mathcal{L}(\mathbf{p}, \mathbf{q}) := \{\mathbf{x} \in \mathbb{R}^n \mid \mathbf{x} = \lambda\mathbf{p} + (1 - \lambda)\mathbf{q}, \lambda \in \mathbb{R}\}. \quad (4)$$

2) *Line segment*: The line segment joining two points $\mathbf{p} \in \mathbb{R}^n$ and $\mathbf{q} \in \mathbb{R}^n$ is given by

$$\mathcal{L}_s(\mathbf{p}, \mathbf{q}) := \{\mathbf{x} \in \mathbb{R}^n \mid \mathbf{x} = \lambda\mathbf{p} + (1 - \lambda)\mathbf{q}, \lambda \in [0, 1]\}. \quad (5)$$

3) *Hyperplane*: The hyperplane passing through $\mathbf{p} \in \mathbb{R}^n$ and orthogonal to $\mathbf{q} \in \mathbb{R}^n \setminus \{\mathbf{0}\}$ is given by

$$\mathcal{P}(\mathbf{p}, \mathbf{q}) := \{\mathbf{x} \in \mathbb{R}^n \mid \mathbf{q}^\top(\mathbf{x} - \mathbf{p}) = 0\}. \quad (6)$$

The hyperplane divides the Euclidean space \mathbb{R}^n into two half-spaces *i.e.*, a closed positive half-space $\mathcal{P}_{\geq}(\mathbf{p}, \mathbf{q})$ and a

closed negative half-space $\mathcal{P}_{\leq}(\mathbf{p}, \mathbf{q})$ which are obtained by substituting '=' with ' \geq ' and ' \leq ' respectively, in the right-hand side of (6). We also use the notations $\mathcal{P}_{>}(\mathbf{p}, \mathbf{q})$ and $\mathcal{P}_{<}(\mathbf{p}, \mathbf{q})$ to denote the open positive and the open negative half-spaces such that $\mathcal{P}_{>}(\mathbf{p}, \mathbf{q}) = \mathcal{P}_{\geq}(\mathbf{p}, \mathbf{q}) \setminus \mathcal{P}(\mathbf{p}, \mathbf{q})$ and $\mathcal{P}_{<}(\mathbf{p}, \mathbf{q}) = \mathcal{P}_{\leq}(\mathbf{p}, \mathbf{q}) \setminus \mathcal{P}(\mathbf{p}, \mathbf{q})$.

D. Hybrid system framework

A hybrid dynamical system [20] is represented using differential and difference inclusions for the state $\xi \in \mathbb{R}^n$ as follows:

$$\begin{cases} \dot{\xi} \in \mathbf{F}(\xi), & \xi \in \mathcal{F}, \\ \xi^+ \in \mathbf{J}(\xi), & \xi \in \mathcal{J}, \end{cases} \quad (7)$$

where the (set-valued) flow map $\mathbf{F} : \mathbb{R}^n \rightrightarrows \mathbb{R}^n$ and jump map $\mathbf{J} : \mathbb{R}^n \rightrightarrows \mathbb{R}^n$ govern continuous and discrete evolution, which can occur, respectively, in the flow set $\mathcal{F} \subset \mathbb{R}^n$ and the jump set $\mathcal{J} \subset \mathbb{R}^n$. The notions of solution ϕ to a hybrid system, hybrid time domain $\text{dom } \phi$, maximal and complete solution are, respectively, as in [20, Def. 2.6, Def. 2.3, Def. 2.7, p.30].

III. PROBLEM FORMULATION

We consider a spherical robot with radius $r \geq 0$ operating in a convex, three-dimensional Euclidean space $\mathcal{W} \subseteq \mathbb{R}^3$. The workspace \mathcal{W} is cluttered with finite number of compact, convex obstacles $\mathcal{O}_i \subset \mathcal{W}, i \in \{1, \dots, b\}, b \in \mathbb{N}$. We define obstacle $\mathcal{O}_0 := (\mathcal{W}^\circ)^c$ as the complement of the interior of the workspace. Collectively, $\mathcal{O}_{\mathcal{W}} = \bigcup_{i \in \mathbb{I}} \mathcal{O}_i$, where $\mathbb{I} = \{0, \dots, b\}$. We make the following workspace feasibility assumption:

Assumption 1. The minimum separation between any pair of obstacles should be greater than or equal to $2(r + \delta)$ *i.e.*, for all $i, j \in \mathbb{I}, i \neq j$, one has

$$d(\mathcal{O}_i, \mathcal{O}_j) := \min_{\mathbf{p} \in \mathcal{O}_i, \mathbf{q} \in \mathcal{O}_j} \|\mathbf{p} - \mathbf{q}\| \geq 2(r + \delta). \quad (8)$$

We then pick an arbitrary value $r_s \in (0, \delta)$ as the minimum distance that the robot should maintain with respect to any obstacle. The obstacle-free workspace is then defined as $\mathcal{W}_0 := \mathcal{W} \setminus \mathcal{O}_{\mathcal{W}}$. Given $y \geq 0$, a y -eroded obstacle-free workspace, \mathcal{W}_y is defined as

$$\mathcal{W}_y := \mathcal{W} \setminus \bigcup_{i \in \mathbb{I}} \mathcal{D}_y^\circ(\mathcal{O}_i) \subseteq \mathcal{W}_0. \quad (9)$$

Hence, \mathcal{W}_{r_a} with $r_a = r + r_s$ is the obstacle-free workspace with respect to the center of the robot *i.e.*, $\mathbf{x} \in \mathcal{W}_{r_a} \iff \mathcal{B}_{r_a}(\mathbf{x}) \subset \mathcal{W}_0$.

The robot is governed by a single integrator dynamics

$$\dot{\mathbf{x}} = \mathbf{u}, \quad (10)$$

where $\mathbf{u} \in \mathbb{R}^3$ is the control input. The task is to design a feedback control law \mathbf{u} such that:

- 1) **Safety**: the obstacle-free workspace \mathcal{W}_{r_a} is forward invariant with respect to the center of the robot,
- 2) **Global Asymptotic Stability**: Any given target location $\mathbf{x}^d \in (\mathcal{W}_{r_a})^\circ$ is a globally asymptotically stable

equilibrium for the closed-loop system. Without loss of generality, we will consider $\mathbf{x}^d = \mathbf{0}$.

IV. HYBRID CONTROL FOR OBSTACLE AVOIDANCE

In the proposed scheme, the robot operates in two modes based on the value of a mode indicator variable $m \in \mathbb{M} := \{0, 1\}$. The *move-to-target* mode ($m = 0$) is adopted when the robot is away from the obstacles and the *obstacle-avoidance* mode ($m = 1$) is adopted when the robot is close to an obstacle obstructing its motion towards the target location. In the *move-to-target* mode, the robot moves straight towards the target location. In the *obstacle-avoidance* mode, the robot navigates around the obstacle while staying within its γ -neighborhood, where $\gamma \in (0, \delta - r_s)$. When the robot operates in the *obstacle-avoidance* mode, the robot's center has a unique closest point on the nearest obstacle. Furthermore, to prevent the robot from getting trapped in a loop around an obstacle, the proposed obstacle-avoidance strategy confines the robot's center to a hyperplane that passes through the target location. It then guides the robot along the boundary to a position where the nearest obstacle no longer intersects with the line segment connecting the robot's center and the target location, as shown in Fig. 1a.

A. Hybrid control design

The proposed hybrid control $\mathbf{u}(\mathbf{x}, \mathbf{h}, \mathbf{a}, m, s)$ is given as

$$\mathbf{u}(\xi) = -\kappa_s(1 - m)\mathbf{x} + \kappa_r m \mathbf{v}(\mathbf{x}, \mathbf{a}), \quad (11a)$$

$$\underbrace{\begin{cases} \dot{\mathbf{h}} = \mathbf{0}, \\ \dot{\mathbf{a}} = \mathbf{0}, \\ \dot{m} = 0 \\ \dot{s} = 1, \end{cases}}_{(\mathbf{x}, \mathbf{h}, \mathbf{a}, m, s) \in \mathcal{F}} \underbrace{\begin{bmatrix} \mathbf{h}^+ \\ \mathbf{a}^+ \\ m^+ \\ s^+ \end{bmatrix}}_{(\mathbf{x}, \mathbf{h}, \mathbf{a}, m, s) \in \mathcal{J}} \in \mathbf{L}(\mathbf{x}, \mathbf{h}, \mathbf{a}, m, s), \quad (11b)$$

where $\kappa_s > 0$, $\kappa_r > 0$, and $\xi = (\mathbf{x}, \mathbf{h}, \mathbf{a}, m, s) \in \mathcal{K} := \mathcal{W}_{r_a} \times \mathcal{W}_{r_a} \times \mathbb{S}^2 \times \mathbb{M} \times \mathbb{R}_{\geq 0}$. The variable \mathbf{h} denotes the *hit point*, which is the location where the robot switches from the *move-to-target* mode to the *obstacle-avoidance* mode. The vector $\mathbf{a} \in \mathbb{S}^2$ is instrumental for the construction of the avoidance control vector $\mathbf{v}(\mathbf{x}, \mathbf{a})$, used in (11a). The scalar variable $s \in \mathbb{R}_{\geq 0}$ allows the robot to switch from the *obstacle-avoidance* mode to the *move-to-target* mode when initially in the *obstacle-avoidance* mode. Details of this switching process are provided later in Section IV-B. The sets \mathcal{F} and \mathcal{J} are the flow and jump sets related to different modes of operation, respectively, whose constructions are provided in Section IV-B. The update law \mathbf{L} , which allows the robot to update the values of the variables \mathbf{h} , \mathbf{a} , m and s based on the current location of the robot with respect to the nearest obstacle and the target location, will be designed later in Section IV-C. Next, we provide the design of the vector $\mathbf{v}(\mathbf{x}, \mathbf{a}) \in \mathbb{R}^3$.

The vector $\mathbf{v}(\mathbf{x}, \mathbf{a})$, used in (11a), is defined as

$$\mathbf{v}(\mathbf{x}, \mathbf{a}) = [\eta(\mathbf{x})\mathbf{I}_3 + (1 - |\eta(\mathbf{x})|)\mathbf{R}(\mathbf{a})]\mathbf{P}(\mathbf{a})\mathbf{x}_\pi \quad (12)$$

where $\mathbf{I}_3 \in \mathbb{R}^{3 \times 3}$ is the identity matrix and $\mathbf{x}_\pi := \mathbf{x} - \Pi(\mathbf{x}, \mathcal{O}_W)$. The location $\Pi(\mathbf{x}, \mathcal{O}_W)$ is the closest point on

the set \mathcal{O}_W from the robot's center \mathbf{x} , as defined in Section II-B. Notice that, since the obstacles $\mathcal{O}_i, i \in \mathbb{I} \setminus \{0\}$ are convex and the parameter $\gamma \in (0, \delta - r_s)$, according to Assumption 1, the robot will have a unique closest point to the obstacles whenever its center is in the $(r_a + \gamma)$ -neighborhood of these obstacles. On the other hand, there may be some locations in the $(r_a + \gamma)$ -neighborhood of the obstacle $\mathcal{O}_0 = (\mathcal{W}^\circ)^c$ for which the uniqueness of the closest point from robot's center to the obstacle \mathcal{O}_0 cannot be guaranteed. However, as discussed later in Remark 1, the design of the flow sets and jump sets guarantees that the obstacle-avoidance control vector $\mathbf{v}(\mathbf{x}, \mathbf{a})$ is never activated in the region $\mathcal{N}_{r_a + \gamma}(\mathcal{O}_0)$.

The rotation matrix $\mathbf{R}(\mathbf{a}) := \mathcal{R}(\frac{\pi}{2}, \mathbf{a}) \in SO(3)$, with $\mathcal{R}(\theta, \mathbf{a})$ being the rotation by an angle θ about the unit vector \mathbf{a} , defined as follows:

$$\mathcal{R}(\theta, \mathbf{a}) := \mathbf{I}_3 + \sin(\theta)\mathbf{a}^\times + (1 - \cos(\theta))(\mathbf{a}^\times)^2,$$

which, for $\theta = \frac{\pi}{2}$, leads to

$$\mathbf{R}(\mathbf{a}) = \mathbf{a}\mathbf{a}^\top + \mathbf{a}^\times,$$

where we used the fact that $(\mathbf{a}^\times)^2 = \mathbf{a}\mathbf{a}^\top - \mathbf{I}_3$, with \mathbf{a}^\times being the skew-symmetric matrix associated to the unit vector $\mathbf{a} = [a_1 \ a_2 \ a_3]^\top$, defined according to (1).

The matrix $\mathbf{P}(\mathbf{a}) \in \mathbb{R}^{3 \times 3}$, which is used in (12), is given by

$$\mathbf{P}(\mathbf{a}) := \mathbf{I}_3 - \mathbf{a}\mathbf{a}^\top, \quad (13)$$

where $\mathbf{a} \in \mathbb{S}^2$. For any vector $\mathbf{x} \in \mathbb{R}^3$, the vector $\mathbf{P}(\mathbf{a})\mathbf{x}$ corresponds to the projection of \mathbf{x} onto the hyperplane orthogonal to \mathbf{a} . As discussed later in Section IV-C, the coordinates of the unit vector \mathbf{a} are updated when the robot switches from the *move-to-target* mode to the *obstacle-avoidance* mode according to the update law $\mathbf{L}(\xi)$, whose design is provided later in Section IV-C.

Finally, the scalar function $\eta(\mathbf{x}) \in [-1, 1]$ is given by

$$\eta(\mathbf{x}) = \begin{cases} -1, & d(\mathbf{x}, \mathcal{O}_W) - r_a \geq \gamma_s, \\ 1 - \frac{d(\mathbf{x}, \mathcal{O}_W) - r_a - \gamma_a}{0.5(\gamma_s - \gamma_a)}, & \gamma_a \leq d(\mathbf{x}, \mathcal{O}_W) - r_a \leq \gamma_s, \\ 1, & d(\mathbf{x}, \mathcal{O}_W) - r_a \leq \gamma_a, \end{cases} \quad (14)$$

where $0 < \gamma_a < \gamma_s < \gamma$. The scalar function η is designed to ensure that the center of the robot remains inside the γ -neighborhood of the r_a -dilated obstacle-occupied workspace $\mathcal{N}_\gamma(\mathcal{D}_{r_a}(\mathcal{O}_W))$ when it operates in the *obstacle-avoidance* mode in the set $\mathcal{N}_\gamma(\mathcal{D}_{r_a}(\mathcal{O}_W))$. This feature allows for the design of the jump set of the *obstacle-avoidance* mode, as discussed later in Section IV-B2, and ensures convergence to the target location, as stated later in Theorem 1. Next, we provide the construction of the flow set \mathcal{F} and the jump set \mathcal{J} used in (11).

B. Geometric construction of the flow and jump sets

When the robot operates in the *move-to-target* mode, its velocity is directed towards the target location. Hence, if the path joining the robot's location and the target is obstructed by an obstacle, let's say \mathcal{O}_i for some $i \in \mathbb{I}$ i.e., $\mathcal{L}_s(\mathbf{x}, \mathbf{0}) \cap \mathcal{D}_{r_a}^\circ(\mathcal{O}_i) \neq \emptyset$, then the center of the robot enters

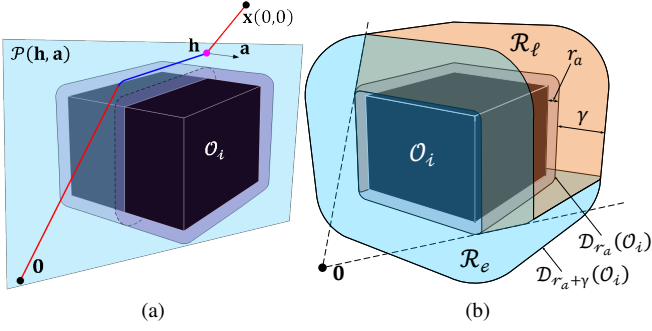


Fig. 1: (a) Robot trajectory moving along the hyperplane $\mathcal{P}(\mathbf{h}, \mathbf{a})$ while avoiding obstacle \mathcal{O}_i . (b) The geometrical representation of the landing region and the exit region.

the $(r_a + \gamma)$ -neighborhood of the obstacle \mathcal{O}_i through the landing region \mathcal{R}_l^i , which is defined as

$$\mathcal{R}_l^i := \{\mathbf{x} \in \mathcal{N}_\gamma(\mathcal{D}_{r_a}(\mathcal{O}_i)) \mid \mathcal{L}_s(\mathbf{x}, \mathbf{0}) \cap \mathcal{D}_{r_a}^\circ(\mathcal{O}_i) \neq \emptyset\}. \quad (15)$$

The union of the landing regions over all obstacles is defined as

$$\mathcal{R}_l := \bigcup_{i \in \mathbb{I}} \mathcal{R}_l^i. \quad (16)$$

Next, we define an exit region \mathcal{R}_e as the part of the γ -neighborhood of the r_a -dilated obstacles that do not belong to the landing region, as shown in Fig. 1b. The exit region \mathcal{R}_e is defined as

$$\mathcal{R}_e = \mathcal{N}_\gamma(\mathcal{D}_{r_a}(\mathcal{O}_W)) \setminus \mathcal{R}_l. \quad (17)$$

Note that when the robot's center at \mathbf{x} belongs to the exit region, the line segment connecting its location to the target location $\mathcal{L}_s(\mathbf{x}, \mathbf{0})$ does not intersect with the interior of the nearest r_a -dilated obstacle. Hence, the robot should move straight towards the target location only if it is in the exit region. Next, we provide the geometric construction of the flow set \mathcal{F} and the jump set \mathcal{J} , used in (11).

1) *Flow and jump sets (move-to-target mode)*: When the robot operating in the move-to-target mode, enters in the landing region \mathcal{R}_l (16), it should switch to the obstacle-avoidance mode to avoid collision. Hence, the jump set of the move-to-target mode for the state \mathbf{x} is defined as

$$\mathcal{J}_0^W := \overline{\mathcal{N}_{\gamma_s}(\mathcal{D}_{r_a}(\mathcal{O}_W))} \cap \mathcal{R}_l, \quad (18)$$

where $\gamma_s \in (0, \gamma)$. For robustness purposes (with respect to noise), we introduce a hysteresis region by allowing the robot, operating in the move-to-target mode inside the $(r_a + \gamma)$ -neighborhood of the set \mathcal{O}_W , to move closer to the set \mathcal{O}_W before switching to the obstacle-avoidance mode.

The flow set of the move-to-target mode for the state \mathbf{x} is then defined as

$$\mathcal{F}_0^W := (\mathcal{W} \setminus (\mathcal{D}_{r_a+\gamma_s}^\circ(\mathcal{O}_W))) \cup \mathcal{R}_e. \quad (19)$$

Notice that the union of the jump set \mathcal{J}_0^W and the flow set \mathcal{F}_0^W covers the robot-centered obstacle-free workspace \mathcal{W}_{r_a} .

The flow set \mathcal{F}_0 and the jump set \mathcal{J}_0 for the move-to-target

mode are given by

$$\begin{aligned} \mathcal{F}_0 &:= \{\xi \in \mathcal{K} \mid \mathbf{x} \in \mathcal{F}_0^W, m = 0\}, \\ \mathcal{J}_0 &:= \{\xi \in \mathcal{K} \mid \mathbf{x} \in \mathcal{J}_0^W, m = 0\}. \end{aligned} \quad (20)$$

2) *Flow and jump sets (obstacle-avoidance mode)*: The robot operates in the obstacle-avoidance mode inside the γ -neighborhood of the obstacle-occupied workspace. Since the robot can safely move straight towards the target location and exit the γ -neighborhood of the nearest obstacle, whenever it is in the exit region (17), it should switch back to the move-to-target mode only if it is in the exit region. To that end, we make use of the hit point \mathbf{h} (i.e., the location of the center of the robot when it switched from the move-to-target mode to the current obstacle-avoidance mode) to define the jump set of the obstacle-avoidance mode \mathcal{J}_1^W for the state \mathbf{x} as follows:

$$\mathcal{J}_1^W := (\mathcal{W} \setminus \mathcal{D}_{r_a+\gamma}^\circ(\mathcal{O}_W)) \cup \mathcal{E}\mathcal{R}^h \cup \mathcal{N}_\gamma(\mathcal{D}_{r_a}(\mathcal{O}_0)) \cup \mathcal{S}_0, \quad (21)$$

where the set $\mathcal{S}_0 := \overline{\mathcal{B}_\gamma(\mathbf{0}) \setminus \mathcal{D}_{r_a}(\mathcal{O}_W)}$. The inclusion of the set \mathcal{S}_0 in the set \mathcal{J}_1^W allows us to ensure the stability of the origin, as stated later in Theorem 1.

For a hit point $\mathbf{h} \in \mathcal{W}_{r_a}$, the set $\mathcal{E}\mathcal{R}^h$ is given by

$$\mathcal{E}\mathcal{R}^h := \{\mathbf{x} \in \mathcal{R}_e \mid \|\mathbf{h}\| - \|\mathbf{x}\| \geq \epsilon\}, \quad (22)$$

with $\epsilon \in (0, \bar{\epsilon}]$ where $\bar{\epsilon}$ is a sufficiently small positive scalar. The set $\mathcal{E}\mathcal{R}^h$ contains the locations from the exit region \mathcal{R}_e which are at least ϵ units closer to the target location than the current hit point \mathbf{h} . Since the obstacles are compact and convex, and the target location $\mathbf{0}$ is within the interior of the obstacle-free workspace \mathcal{W}_{r_a} , it is possible to guarantee the existence of the parameter $\bar{\epsilon}$ such that the intersection set $\mathcal{E}\mathcal{R}^h \cap \mathcal{N}_\gamma(\mathcal{D}_{r_a}(\mathcal{O}_i))$ is non-empty for every $\mathbf{h} \in \mathcal{J}_0^W \cap \mathcal{N}_\gamma(\mathcal{D}_{r_a}(\mathcal{O}_i))$ for each $i \in \mathbb{I}$, as stated in the following lemma:

Lemma 1. Let Assumption 1 hold. Then, for every $\mathbf{h} \in \mathcal{J}_0^W \cap \mathcal{N}_\gamma(\mathcal{D}_{r_a}(\mathcal{O}_i))$, there exists $\bar{\epsilon} > 0$ such that for any $\epsilon \in (0, \bar{\epsilon}]$ the set $\mathcal{E}\mathcal{R}^h \cap \mathcal{N}_\gamma(\mathcal{D}_{r_a}(\mathcal{O}_i)) \neq \emptyset$, where the set $\mathcal{E}\mathcal{R}^h$ is defined in (22).

Proof. See Appendix IX-A. \square

According to (21) and (22), the robot operating in the obstacle-avoidance mode, can switch to the move-to-target mode when its center belongs to the exit region \mathcal{R}_e and the target location $\mathbf{0}$ is at least ϵ units closer to \mathbf{x} than the current hit point \mathbf{h} .

The flow set of the obstacle-avoidance mode for the state \mathbf{x} i.e., \mathcal{F}_1^W is defined as follows:

$$\mathcal{F}_1^W := \overline{\mathcal{N}_\gamma(\mathcal{D}_{r_a}(\mathcal{O}_W)) \setminus (\mathcal{E}\mathcal{R}^h \cup \mathcal{N}_\gamma(\mathcal{D}_{r_a}(\mathcal{O}_0)))}. \quad (23)$$

Notice that the union of the jump set (21) and the flow set (23) exactly covers the robot-centered obstacle-free workspace \mathcal{W}_{r_a} .

Remark 1. Given that the workspace \mathcal{W} is both convex and compact, there may exist some locations $\mathbf{x} \in \mathcal{N}_\gamma(\mathcal{D}_{r_a}(\mathcal{O}_0))$ from which the nearest point to the robot's center on the obstacle $\mathcal{O}_0 = (\mathcal{W}^\circ)^c$ is not unique. This scenario prevents the implementation of the obstacle-avoidance term $\mathbf{v}(\mathbf{x}, \mathbf{a})$ in

the control law, at such locations. However, by excluding the set $\mathcal{N}_\gamma(\mathcal{D}_{r_a}(\mathcal{O}_0))$ from the set $\mathcal{F}_1^\mathcal{W}$, as defined in (23), it is ensured that the *obstacle-avoidance* mode is never activated within the set $\mathcal{N}_\gamma(\mathcal{D}_{r_a}(\mathcal{O}_0))$.

The flow set \mathcal{F}_1 and the jump set \mathcal{J}_1 for the *obstacle-avoidance* mode are given by

$$\begin{aligned}\mathcal{F}_1 &:= \{\xi \in \mathcal{K} | \mathbf{x} \in \mathcal{F}_1^\mathcal{W}, m = 1, s \notin (s_0, s_0 + \delta_s)\}, \\ \mathcal{J}_1 &:= \mathcal{J}_\mathbf{x} \cup \mathcal{J}_s,\end{aligned}\quad (24)$$

where $\mathcal{J}_\mathbf{x} := \{\xi \in \mathcal{K} | m = 1, \mathbf{x} \in \mathcal{J}_1^\mathcal{W}\}$ and $\mathcal{J}_s := \{\xi \in \mathcal{K} | m = 1, s = [s_0, s_0 + \delta_s]\}$ with $s_0 \in \mathbb{R}_{\geq 0}$ being the initial value of the state s , i.e., $s(0, 0) = s_0$, and $0 < \delta_s < \tau_s$ for some $\tau_s > 0$.

Remark 2. The definition of sets in (24) enables the control to immediately switch to the *move-to-target* mode if it is initialized in the *obstacle-avoidance* mode (i.e., $\xi(0, 0) \in \mathcal{J}_1$). This ensures that the *hit point* \mathbf{h} always belongs to the set $\mathcal{J}_0^\mathcal{W}$ before the robot starts moving in the *obstacle-avoidance* mode, thus guaranteeing the existence of the parameter $\bar{\epsilon}$, as stated in Lemma 1.

Finally, the flow set \mathcal{F} and the jump set \mathcal{J} , used in (11), are defined as

$$\mathcal{F} := \bigcup_{m \in \mathbb{M}} \mathcal{F}_m, \quad \mathcal{J} := \bigcup_{m \in \mathbb{M}} \mathcal{J}_m, \quad (25)$$

where $\mathcal{F}_0, \mathcal{J}_0$ defined in (20) for $m = 0$ and in (24) for $m = 1$. Next, we provide the update law $\mathbf{L}(\mathbf{x}, \mathbf{h}, \mathbf{a}, m, s)$ used in (11b).

C. Update law $\mathbf{L}(\mathbf{x}, \mathbf{h}, \mathbf{a}, m, s)$

The update law $\mathbf{L}(\xi)$, used in (11b), updates the value of the *hit point* \mathbf{h} , the unit vector \mathbf{a} , the mode indicator m and the variable s when the state $(\mathbf{x}, \mathbf{h}, \mathbf{a}, m, s)$ belongs to the jump set \mathcal{J} defined in (25) and is given by

$$\mathbf{L}(\xi) = \begin{cases} \mathbf{L}_0(\xi), & \xi \in \mathcal{J}_0, \\ \mathbf{L}_1(\xi), & \xi \in \mathcal{J}_1. \end{cases} \quad (26)$$

When the state ξ enters in the jump set \mathcal{J}_0 (20), the update law $\mathbf{L}_0(\mathbf{x}, \mathbf{h}, \mathbf{a}, 0, s)$ is given as

$$\mathbf{L}_0(\mathbf{x}, \mathbf{h}, \mathbf{a}, 0, s) = \left\{ \begin{bmatrix} \mathbf{x} \\ \mathbf{a}' \\ 1 \\ s + \tau_s \end{bmatrix}, \mathbf{a}' \in \mathbf{A}(\mathbf{x}) \right\}, \quad (27)$$

where $\tau_s > 0$. Given $\mathbf{x} \in \mathcal{N}_\gamma(\mathcal{D}_{r_a}(\mathcal{O}_\mathcal{W}))$, the set-valued mapping $\mathbf{A} : \mathbb{R}^3 \rightrightarrows \mathbb{S}^2$ is defined as

$$\mathbf{A}(\mathbf{x}) = \begin{cases} \mathbf{q} \in \mathcal{P}^\perp(\mathbf{x}), & \mathbf{x}^\times \mathbf{x}_\pi = \mathbf{0}, \\ \mathbf{q} \in \pm \frac{\mathbf{x}^\times \mathbf{x}_\pi}{\|\mathbf{x}^\times \mathbf{x}_\pi\|}, & \mathbf{x}^\times \mathbf{x}_\pi \neq \mathbf{0}, \end{cases} \quad (28)$$

where for any $\mathbf{p} \in \mathbb{R}^3$, the set $\mathcal{P}^\perp(\mathbf{p})$, which is defined as

$$\mathcal{P}^\perp(\mathbf{p}) := \{\mathbf{q} \in \mathbb{S}^2 | \mathbf{q}^\top \mathbf{p} = 0\}, \quad (29)$$

contains unit vectors that are perpendicular to the vector \mathbf{p} .

According to (27), when the robot switches from the *move-to-target* mode to the *obstacle-avoidance* mode, the coordinates of the *hit point* \mathbf{h} get updated to the current value of

\mathbf{x} . Moreover, according to (28), the unit vector \mathbf{a} is updated such that it is perpendicular to the vector \mathbf{h} and the resulting hyperplane $\mathcal{P}(\mathbf{h}, \mathbf{a})$ intersects with the interior of the nearest r_a -dilated obstacle. Since the target location $\mathbf{0} \in \mathcal{P}(\mathbf{h}, \mathbf{a})$ and the *hit point* $\mathbf{h} \in \mathcal{J}_0^\mathcal{W}$, the hyperplane intersects with both the *landing region* \mathcal{R}_l and the *exit region* \mathcal{R}_e associated with the nearest obstacle. This feature is then used to ensure that the robot, operating in the *obstacle-avoidance* mode, always enters in the *move-to-target* mode. This allows one to ensure global convergence to the target location, as stated later in Theorem 1.

When the state ξ enters in the jump set \mathcal{J}_1 , defined in (24), the update law $\mathbf{L}_1(\mathbf{x}, \mathbf{h}, \mathbf{a}, 1, s)$ is given by

$$\mathbf{L}_1(\mathbf{x}, \mathbf{h}, \mathbf{a}, 1, s) = \begin{bmatrix} \mathbf{h} \\ \mathbf{a} \\ 0 \\ s + \tau_s \end{bmatrix}. \quad (30)$$

According to (30), when the robot switches from the *obstacle-avoidance* mode to the *move-to-target* mode, the coordinates of the *hit point* \mathbf{h} and the unit vector \mathbf{a} remain unchanged.

Remark 3. Since the parameter $\gamma \in (r_s, \delta - r_s)$, according to Assumption 1, the $(r_a + \gamma)$ -dilated obstacles $\mathcal{D}_{r_a + \gamma}(\mathcal{O}_i)$, $\forall i \in \mathbb{I}$, are disjoint, and the target location $\mathbf{0} \in \mathcal{W}_{r_a + \gamma}^\circ$. Furthermore, according to (23), the set $\mathcal{F}_1^\mathcal{W}$ is contained within the region $\mathcal{D}_{r_a + \gamma}(\mathcal{O}_\mathcal{W})$. Hence, the proposed control law enables the robot to avoid one obstacle at a time.

This concludes the design of the proposed hybrid feedback controller (11). Next, we analyze the safety, stability and convergence properties of the proposed hybrid feedback controller.

V. STABILITY ANALYSIS

The hybrid closed-loop system resulting from the hybrid feedback control law (11) is given by

$$\begin{aligned} \dot{\mathbf{x}} &= \mathbf{u}(\xi) & \mathbf{x}^+ &= \mathbf{x} \\ \dot{\mathbf{h}} &= \mathbf{0} & \mathbf{h}^+ &= \mathbf{h} \\ \dot{\mathbf{a}} &= \mathbf{0} & \mathbf{a}^+ &= \mathbf{a} \\ \dot{m} &= 0 & m^+ &= m \\ \dot{s} &= 1 & s^+ &= s \end{aligned} \quad \begin{cases} \underbrace{\begin{bmatrix} \mathbf{x}^+ \\ \mathbf{h}^+ \\ \mathbf{a}^+ \\ m^+ \\ s^+ \end{bmatrix}}_{\xi^+ = \mathbf{F}(\xi), \xi \in \mathcal{F}}, & \underbrace{\begin{bmatrix} \mathbf{h}^+ \\ \mathbf{a}^+ \\ m^+ \\ s^+ \end{bmatrix}}_{\xi^+ \in \mathbf{J}(\xi), \xi \in \mathcal{J}}, \end{cases} \in \mathbf{L}(\xi) \quad (31)$$

where $\mathbf{u}(\xi)$ is defined in (11a), and the update law $\mathbf{L}(\xi)$ is provided in (26). Definitions of the flow set \mathcal{F} and the jump set \mathcal{J} are provided in (25). Next, we analyze the hybrid closed-loop system (31) in terms of forward invariance of the obstacle-free state space \mathcal{K} , along with the stability properties of the target set

$$\mathcal{A} := \{\xi \in \mathcal{K} | \mathbf{x} = \mathbf{0}\}. \quad (32)$$

The next lemma shows that the hybrid closed-loop system (31) satisfies the hybrid basic conditions [20, Assumption 6.5], which guarantees the well-posedness of the hybrid closed-loop system.

Lemma 2. The hybrid closed-loop system (31) with data $(\mathcal{F}, \mathbf{F}, \mathcal{J}, \mathbf{J})$ satisfies the following hybrid basic conditions:

- 1) the flow set \mathcal{F} and the jump set \mathcal{J} , defined in (25), are closed subsets of $\mathbb{R}^3 \times \mathbb{R}^3 \times \mathbb{R}^3 \times \mathbb{R} \times \mathbb{R}$.
- 2) the flow map \mathbf{F} , defined in (31), is outer semicontinuous and locally bounded relative to \mathcal{F} , $\mathcal{F} \subset \text{dom } \mathbf{F}$, and $\mathbf{F}(\xi)$ is convex for every $\xi \in \mathcal{F}$.
- 3) the jump map \mathbf{J} , defined in (31), is outer semicontinuous and locally bounded relative to \mathcal{J} , $\mathcal{J} \subset \text{dom } \mathbf{J}$.

Proof. See Appendix IX-B. \square

For safe autonomous navigation, the state \mathbf{x} must always evolve within the obstacle-free workspace \mathcal{W}_{r_a} , defined in (9). This is equivalent to having the set \mathcal{K} forward invariant for the hybrid closed-loop system (31). This is stated in the next Lemma.

Lemma 3. Under Assumption 1, for the hybrid closed-loop system (31), the obstacle-free set $\mathcal{K} := \mathcal{W}_{r_a} \times \mathcal{W}_{r_a} \times \mathbb{S}^2 \times \mathbb{M} \times \mathbb{R}_{\geq 0}$ is forward invariant.

Proof. See Appendix IX-C. \square

Next, we provide one of our main results which establishes the fact that for all initial conditions in the obstacle-free set \mathcal{K} , the proposed hybrid controller not only ensures safe navigation but also guarantees global asymptotic stability of the target location at the origin.

Theorem 1. Under Assumption 1, for the hybrid closed-loop system (31), the following holds true:

- i) the obstacle-free set \mathcal{K} is forward invariant,
- ii) the target set \mathcal{A} is globally asymptotically stable over the set \mathcal{K} ,
- iii) the number of jumps is finite.

Proof. See Appendix IX-D. \square

VI. IMPLEMENTATION PROCEDURE

We consider a workspace with convex obstacles that satisfies Assumption 1 with some $\delta > 0$. The target location is set at the origin within the interior of the obstacle-free workspace $\mathcal{W}_{r_a}^\circ$. The center of the robot is initialized in the obstacle-free workspace \mathcal{W}_{r_a} . The variables $\mathbf{h}, \mathbf{a}, m$ and s are initialized in the sets $\mathcal{W}_{r_a}, \mathbb{S}^2, \mathbb{M}$ and $\mathbb{R}_{\geq 0}$, respectively. Since $\gamma \in (0, \delta - r_s)$, the algorithm to avoid one obstacle at a time, as discussed in Remark 3. The parameters γ_a and γ_s are set to satisfy $0 < \gamma_a < \gamma_s < \gamma$. A sufficiently small value for $\bar{\epsilon}$ is selected as stated in Lemma 1, and the parameter $\epsilon \in (0, \bar{\epsilon}]$. We set a sensing radius $R_s > r_a + \gamma$ such that the robot can detect the boundary of the obstacles within its line-of-sight inside the region $\mathcal{B}_{R_s}(\mathbf{x})$.

When the control input is initialized in the *move-to-target* mode, according to (11a), it steers the robot straight towards the origin. The robot should constantly measure the distance between its center and the surrounding obstacles to identify whether the state ξ has entered in the jump set \mathcal{J}_0 of the *move-to-target* mode. To do this, the robot needs to identify the set $\partial\mathcal{O}$ which contains the locations from the boundary of the surrounding obstacles that are less than R_s units away from the center of the robot and have clear line-of-sight to

the center of the robot, where $R_s > r_a + \gamma$ represents sensing radius. In other words, the set $\partial\mathcal{O}$ is defined as

$$\partial\mathcal{O} = \{\mathbf{p} \in \partial\mathcal{O}_{\mathcal{W}} \mid \|\mathbf{x} - \mathbf{p}\| \leq R_s, \mathcal{L}_s(\mathbf{x}, \mathbf{p}) \cap \mathcal{D}_{r_a}^\circ(\mathcal{O}_{\mathcal{W}}) = \emptyset\}. \quad (33)$$

Then, one can obtain the distance between the robot's center and the surrounding obstacles by evaluating $d(\mathbf{x}, \partial\mathcal{O})$ according to Section II-B. If $d(\mathbf{x}, \partial\mathcal{O}) \leq r_a + \gamma_s$, the algorithm should identify whether the robot can move straight towards the target location without colliding with the nearest obstacle. In other words, the algorithm should evaluate whether the center of the robot belongs to the *landing* region \mathcal{R}_l , defined in (15), associated with the nearest obstacle. To that end, the algorithm identifies the set $\partial\mathcal{O}_c \subset \partial\mathcal{O}$ which contains the locations from the set $\partial\mathcal{O}$ that belong to the boundary of the closest obstacle. Let \mathcal{O}_i for some $i \in \mathbb{I}$ be the closest obstacle to the center of the robot, then the set $\partial\mathcal{O}_c$ is defined as

$$\partial\mathcal{O}_c = \partial\mathcal{O}_i \cap \partial\mathcal{O}. \quad (34)$$

Once the set $\partial\mathcal{O}_c$ has been identified, one needs to determine whether the center of the robot \mathbf{x} belongs to the *landing* region \mathcal{R}_l by evaluating the intersection between the set $\partial\mathcal{O}_c$ and the set $\mathcal{D}_{r_a}^\circ(\mathcal{L}_s(\mathbf{x}, \mathbf{0}))$. If $\partial\mathcal{O}_c \cap \mathcal{D}_{r_a}^\circ(\mathcal{L}_s(\mathbf{x}, \mathbf{0})) \neq \emptyset$, then the center of the robot belongs to the set \mathcal{R}_l and, as per (18) and (20), the state ξ has entered in the jump set of the *move-to-target* mode \mathcal{J}_0 . Otherwise, the robot continues to operate in the *move-to-target* mode.

When the state ξ enters in the jump set of the *move-to-target* mode \mathcal{J}_0 , the algorithm updates the state ξ as per (27) and (31), and the control input switches to the *obstacle-avoidance* mode. According to Lemma 4, when the robot operates in the *obstacle-avoidance* mode, it stays inside the γ -neighborhood of the closest obstacle. As the robot operates in the *obstacle-avoidance* mode, the algorithm continuously evaluates the intersection $\partial\mathcal{O}_c \cap \mathcal{D}_{r_a}^\circ(\mathcal{L}_s(\mathbf{x}, \mathbf{0}))$ to check whether the center of the robot has entered in the *exit* region \mathcal{R}_e . If $\partial\mathcal{O}_c \cap \mathcal{D}_{r_a}^\circ(\mathcal{L}_s(\mathbf{x}, \mathbf{0})) = \emptyset$, then the center of the robot belongs to the exit region \mathcal{R}_e . Additionally, if the target location is at least ϵ units closer to \mathbf{x} than to the current *hit point* \mathbf{h} , then it implies that $\xi \in \mathcal{J}_1$. Then the algorithm updates the value of the variables m and s as per (30) and the control input switches to the *move-to-target* mode.

Finally, if the control input is initialized in the *obstacle-avoidance* mode, according to (24), the state $\xi(0, 0)$ belongs to the jump set of the *obstacle-avoidance* mode \mathcal{J}_1 . As a result, according to (30) the algorithm updates the value of the variables $\mathbf{h}, \mathbf{a}, m$ and s , and switches the control input to the *move-to-target* mode.

The above-mentioned implementation procedure is summarised in Algorithm 1.

VII. SIMULATION RESULTS

We compare our approach with the separating hyperplane method developed in [12] which can be implemented in *a priori* unknown environments using information from a range-bearing sensor mounted on the robot. However, unlike our approach, it only works for strongly convex obstacles [12, Assumption 2]. The workspace contains two obstacles, an

Algorithm 1 Implementation of the proposed hybrid control law (11) in *a priori* unknown environment.

```

1: Set target location at the origin  $\mathbf{0}$ .
2: Initialize  $\mathbf{x}(0,0) \in \mathcal{W}_{r_a}$ ,  $\mathbf{h}(0,0) \in \mathcal{W}_{r_a}$ ,  $\mathbf{a}(0,0) \in \mathbb{S}^2$ ,
    $m(0,0) \in \mathbb{M}$  and  $s(0,0) \in \mathbb{R}_{\geq 0}$ . Choose sufficiently small
   value of  $\bar{\epsilon}$  according to Lemma 1, and initialize  $\epsilon \in (0, \bar{\epsilon}]$ .
   Identify the parameter  $\delta$ , as discussed in Assumption 1,
   and set parameters  $\gamma, \gamma_s$  and  $\gamma_a$  such that  $0 < \gamma_a < \gamma_s < \gamma < \delta - r_s$ .
   Choose  $R_s > r_a + \gamma$ , used in (33). Set  $\tau_s > 0$ 
   and  $\delta_s \in (0, \tau_s)$ .
3: Measure  $\mathbf{x}$  and the set  $\partial\mathcal{O}$  as defined in (33).
4: if  $m = 0$ , then
5:   if  $d(\mathbf{x}, \partial\mathcal{O}) \leq r_a + \gamma_s$ , then
6:     Identify the set  $\partial\mathcal{O}_c \subset \partial\mathcal{O}$  as defined in (34).
7:     if  $\partial\mathcal{O}_c \cap \mathcal{D}_{r_a}^\circ(\mathcal{L}_s(\mathbf{x}, \mathbf{0})) \neq \emptyset$ , then
8:       Update  $\xi \leftarrow \mathbf{J}(\xi)$  using (27) and (31).
9:     end if
10:   end if
11: end if
12: if  $m = 1$ , then
13:   if  $s = s(0,0)$ , then
14:     Update  $\xi \leftarrow \mathbf{J}(\xi)$  using (30) and (31).
15:   else
16:     if  $d(\mathbf{x}, \partial\mathcal{O}) \leq r_a + \gamma$ , then
17:       Identify the set  $\partial\mathcal{O}_c \subset \partial\mathcal{O}$  as defined in (34).
18:       if  $\partial\mathcal{O}_c \cap \mathcal{D}_{r_a}^\circ(\mathcal{L}_s(\mathbf{x}, \mathbf{0})) = \emptyset$ , then
19:         if  $\|\mathbf{x}\| \leq \|\mathbf{h}\| - \epsilon$ , then
20:           Update  $\xi \leftarrow \mathbf{J}(\xi)$  using (30) and (31).
21:         end if
22:       end if
23:     else
24:       Update  $\xi \leftarrow \mathbf{J}(\xi)$  using (30) and (31).
25:     end if
26:   end if
27: end if
28: Execute  $\mathbf{F}(\xi)$  given (11), used in (31).
29: Go to step 3.

```

ellipsoidal obstacle (strongly convex) and a polygonal obstacle that does not satisfy [12, Assumption 2]. The robot's radius is set to $0.2m$, with a minimum safety distance $r_s = 0.1m$ and $\gamma = 0.5m$. The gains $\kappa_s = 0.4$ and $\kappa_r = 2$ are used in (11a), while the sensing radius $R_s = 2m$ is used in (33), and $\epsilon = 0.5m$ in (22).

In Fig. 2a, the dotted portion of the trajectory represents the motion of the robot in the *move-to-target* mode, whereas the solid portion corresponds to the motion in the *obstacle-avoidance* mode. The proposed hybrid feedback controller guarantees safe, global asymptotic convergence to the target location at the origin starting from eight different initial locations as shown in Fig. 2a. In contrast, the separating hyperplane approach generates trajectories that converge to an undesired equilibrium (local minimum), as seen in Fig. 2b. The complete simulation video is available at².

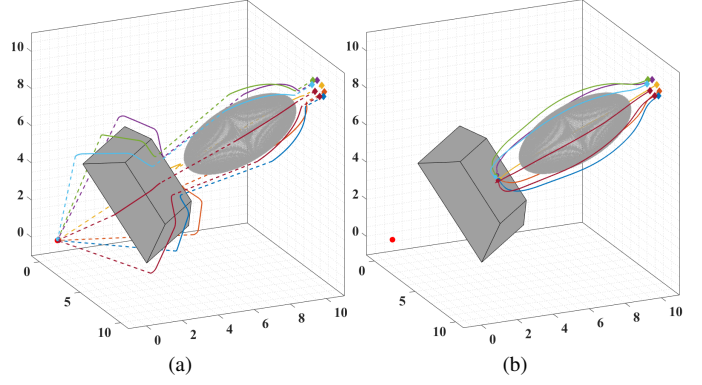


Fig. 2: (a) Trajectories obtained using our proposed approach. (b) Trajectories obtained using the separating hyperplane approach [12].

VIII. CONCLUSION

We propose a hybrid feedback controller for safe autonomous robot navigation in three-dimensional environments with arbitrarily-shaped convex obstacles. These obstacles may have nonsmooth boundaries, large sizes, and can be placed arbitrarily, provided they meet certain mild disjointness requirements, as per Assumption 1. The proposed hybrid controller guarantees global asymptotic stability of the target location in the obstacle-free workspace. The obstacle-avoidance component of the control law relies on the projection of the robot's center onto the nearest obstacle, enabling applications in *a priori* unknown environments, as discussed in Section VI. The proposed hybrid feedback control law generates discontinuous vector fields when switching between modes. Incorporating a smoothing mechanism in our proposed hybrid feedback would be an interesting practical extension. Moreover, extending our approach to second-order robot dynamics navigating in three-dimensional environments with non-convex obstacles, would be an interesting future work.

IX. APPENDIX

A. Proof of Lemma 1

Since the target location at the origin $\mathbf{0}$ belongs to the interior of the obstacle-free workspace $\mathcal{W}_{r_a}^\circ$, there exists some distance between the target location and the r_a -dilated obstacle $\mathcal{D}_{r_a}(\mathcal{O}_i)$. In other words, since $\mathbf{0} \in \mathcal{W}_{r_a}^\circ$, there exists $\bar{\delta} > 0$ such that $d(\mathbf{0}, \mathcal{D}_{r_a}(\mathcal{O}_i)) = \bar{\delta}$. Notice that, since the workspace satisfies Assumption 1, according to (18), the set $\mathcal{J}_0^\mathcal{W} \cap \mathcal{N}_\gamma(\mathcal{D}_{r_a}(\mathcal{O}_i))$ belongs to the *landing* region associated with obstacle \mathcal{O}_i i.e., $(\mathcal{J}_0^\mathcal{W} \cap \mathcal{N}_\gamma(\mathcal{D}_{r_a}(\mathcal{O}_i))) \subset \bar{\mathcal{R}}_l^i$. According to (15), the location $\Pi(\mathbf{0}, \mathcal{D}_{r_a}(\mathcal{O}_i))$ does not belong to the set $\bar{\mathcal{R}}_l^i$. As a result, one has $d(\mathbf{0}, \bar{\mathcal{R}}_l^i) > \bar{\delta}$. Hence, it is clear that $\mathcal{B}_{\bar{\delta}}(\mathbf{0}) \cap \mathcal{N}_\gamma(\mathcal{D}_{r_a}(\mathcal{O}_i)) \cap \mathcal{J}_0^\mathcal{W} = \emptyset$, where $\mathcal{B}_{\bar{\delta}}(\mathbf{0}) \cap \mathcal{N}_\gamma(\mathcal{D}_{r_a}(\mathcal{O}_i)) \neq \emptyset$. Hence, one can set $\bar{\epsilon} \in (0, d(\mathbf{0}, \bar{\mathcal{R}}_l^i) - \bar{\delta}]$ to ensure that $\mathcal{E}\mathcal{R}^h \cap \mathcal{N}_\gamma(\mathcal{D}_{r_a}(\mathcal{O}_i)) \neq \emptyset$ for all $\mathbf{h} \in \mathcal{J}_0^\mathcal{W} \cap \mathcal{N}_\gamma(\mathcal{D}_{r_a}(\mathcal{O}_i))$, for any $\epsilon \in (0, \bar{\epsilon}]$, where the set $\mathcal{E}\mathcal{R}^h$ is defined in (22).

²[Online]. Available: <https://youtu.be/xihWpec8kis>

B. Proof of Lemma 2

The flow set \mathcal{F} and the jump set \mathcal{J} , defined in (25) are by construction closed subsets of $\mathbb{R}^3 \times \mathbb{R}^3 \times \mathbb{R}^3 \times \mathbb{R} \times \mathbb{R}$. Hence, condition 1 in Lemma 2 is satisfied.

Since the flow map $\mathbf{F}(\xi)$ is defined for all $\xi \in \mathcal{F}$, $\mathcal{F} \subset \text{dom } \mathbf{F}$. The flow map \mathbf{F} , given in (31), is continuous on \mathcal{F}_0 . Next, we verify the continuity of \mathbf{F} on \mathcal{F}_1 . Since $\gamma \in (0, \delta - r_s)$, the sets $\mathcal{N}_\gamma(\mathcal{D}_{r_a}(\mathcal{O}_i))$, for all $i \in \mathbb{I}$, are disjoint. Since obstacles $\mathcal{O}_i, i \in \mathbb{I} \setminus \{0\}$ are convex, for all $\mathbf{x} \in \mathcal{N}_\gamma(\mathcal{D}_{r_a}(\mathcal{O}_i)), i \in \mathbb{I} \setminus \{0\}$, the closest point from \mathbf{x} on the boundary of the nearest obstacle $\Pi(\mathbf{x}, \mathcal{O}_i)$ is unique. Furthermore, according to (23), the set $\mathcal{F}_1^\mathcal{W} \subset \bigcup_{i \in \mathbb{I} \setminus \{0\}} \mathcal{N}_\gamma(\mathcal{D}_{r_a}(\mathcal{O}_i))$. Hence, according to [21, Lemma 4.1] and (23), $\Pi(\mathbf{x}, \mathcal{O}_\mathcal{W})$ is continuous for all $\mathbf{x} \in \mathcal{F}_1^\mathcal{W}$. Hence, the obstacle-avoidance control vector $\kappa_r \mathbf{v}(\mathbf{x}, \mathbf{a})$, used in (11a), is continuous for all $\mathbf{x} \in \mathcal{F}_1^\mathcal{W}$ with the unit vector \mathbf{a} chosen as per (27). As a result, \mathbf{F} is continuous on \mathcal{F}_1 and as such it is continuous on \mathcal{F} . This shows fulfillment of condition 2 in Lemma 2.

Since the jump map $\mathbf{J}(\xi)$ is defined for all $\xi \in \mathcal{J}$, $\mathcal{J} \subset \text{dom } \mathbf{J}$. The jump map \mathbf{J} , defined in (31), is single-valued on \mathcal{J}_1 . Hence, according to [20, Definition 5.9 and 5.14], the jump map \mathbf{J} is outer semicontinuous and locally bounded relative to \mathcal{J}_1 .

Finally, we prove that the jump map \mathbf{J} is outer semicontinuous and locally bounded relative to \mathcal{J}_0 . According to (27) and (31), the jump map \mathbf{J} is single-valued for the state vector $(\mathbf{x}, \mathbf{h}, m, s)$ on \mathcal{J}_0 . Consider the jump map \mathbf{J} for the state \mathbf{a} on \mathcal{J}_0 . We show that the set-valued mapping $\mathbf{A} : \mathbb{R}^3 \rightrightarrows \mathbb{S}^2$, used in (27), is outer semicontinuous and locally bounded relative to $\mathcal{J}_0^\mathcal{W}$. To that end, consider any sequence $\{\mathbf{q}_i\}_{i \in \mathbb{N}} \subset \mathcal{J}_0^\mathcal{W}$ that converges to some $\mathbf{q} \in \mathcal{J}_0^\mathcal{W}$. According to (28), $\mathbf{p}_i \in \mathbf{A}(\mathbf{q}_i) \in \mathcal{P}^\perp(\mathbf{q}_i) \cap \mathcal{P}^\perp(\mathbf{q}_i - \Pi(\mathbf{q}_i, \mathcal{O}_\mathcal{W}))$, where for all $\mathbf{q}_i \in \mathcal{J}_0^\mathcal{W}$, $\Pi(\mathbf{q}_i, \mathcal{O}_\mathcal{W})$ is unique. Let us assume that the sequence $\{\mathbf{p}_i\}_{i \in \mathbb{N}}$ converges to some $\mathbf{p} \in \mathbb{S}^2$. Note that $\mathbf{p}_i^\top \mathbf{q}_i = 0$ and $\mathbf{p}_i^\top (\mathbf{q}_i - \Pi(\mathbf{q}_i, \mathcal{O}_\mathcal{W})) = 0$ for all $i \in \mathbb{N}$. Additionally, according to (28), when $\mathbf{q}_i^\times (\mathbf{q}_i - \Pi(\mathbf{q}_i, \mathcal{O}_\mathcal{W})) = \mathbf{0}$, one has $\mathbf{p}_i \in \mathcal{P}^\perp(\mathbf{q}_i)$. Therefore, one can conclude that $\mathbf{p}^\top \mathbf{q} = 0$ and $\mathbf{p}^\top (\mathbf{q} - \Pi(\mathbf{q}, \mathcal{O}_\mathcal{W})) = 0$ and as such $\mathbf{p} \in \mathbf{A}(\mathbf{q})$. Hence, according [20, Definition 5.9], the mapping \mathbf{A} is outer semicontinuous relative to $\mathcal{J}_0^\mathcal{W}$. Since $\text{rge } \mathbf{A} = \mathbb{S}^2 \subset \mathbb{R}^3$ is bounded, according to [20, Definition 5.14], the set-valued mapping \mathbf{A} is locally bounded, where the range of \mathbf{A} is defined as per [20, Definition 5.8]. Hence, \mathbf{J} is outer semi-continuous and locally bounded relative to \mathcal{J}_0 . This shows the fulfillment of condition 3 in Lemma 2.

C. Proof sketch for Lemma 3

Since the proposed hybrid closed-loop system (31) satisfies the hybrid basic conditions outlined in Lemma 2, we make use of [20, Proposition 6.10] to show the forward invariance of \mathcal{K} . Specifically, we verify the satisfaction of the following viability condition:

$$\mathbf{F}(\xi) \cap \mathbf{T}_\mathcal{F}(\xi) \neq \emptyset, \forall \xi \in \mathcal{F} \setminus \mathcal{J}, \quad (35)$$

which allows us to establish the completeness of the solution ξ to the hybrid closed-loop system (31). In (35), $\mathbf{T}_\mathcal{F}(\xi)$ represents the tangent cone to the set \mathcal{F} at ξ .

According to [20, Proposition 6.10], since (35) holds for all $\xi \in \mathcal{F} \setminus \mathcal{J}$, there exists a maximal solution to (31) for each initial condition in \mathcal{K} . Finite escape time can only occur through flow, but it cannot occur for \mathbf{x} in the set $\mathcal{F}_1^\mathcal{W}$, as this set is bounded by definition (23), nor for \mathbf{x} in the set $\mathcal{F}_0^\mathcal{W}$, as this would make $\mathbf{x}^\top \mathbf{x}$ grow unbounded, contradicting the fact that $\frac{d}{dt}(\mathbf{x}^\top \mathbf{x}) \leq 0$ according to the definition of $\mathbf{u}(\mathbf{x}, \mathbf{h}, \mathbf{a}, 0, s)$. Therefore, all maximal solutions do not have finite escape times, and Claim (b) in [20, Proposition 6.10] does not hold.

According to (20) and (24), by construction, we have $\mathcal{F}_m \cup \mathcal{J}_m = \mathcal{K}$ for each $m \in \mathbb{M}$. Therefore, using (27), (30) and (31), it can be verified that $\mathbf{L}(\xi) \in \mathcal{F} \cup \mathcal{J} = \mathcal{K}$ for every $\xi \in \mathcal{K}$. As a result, Claim (c) in [20, Proposition 6.10] does not apply. Therefore, Claim (a) in [20, Proposition 6.10] holds. In other words, all maximal solutions to the hybrid closed-loop system (31) are complete, implying the forward invariance of the obstacle-free set \mathcal{K} .

D. Proof of Theorem 1

Forward invariance and stability: The forward invariance of the obstacle-free set \mathcal{K} , for the hybrid closed-loop system (31), is immediate from Lemma 3. We next prove the stability of \mathcal{A} using [20, Definition 7.1].

Since $\mathbf{0} \in (\mathcal{W}_{r_a})^\circ$, there exists $\mu_1 > 0$ such that $\mathcal{B}_{\mu_1}(\mathbf{0}) \cap (\mathcal{D}_{r_a}(\mathcal{O}_\mathcal{W}))^\circ = \emptyset$. According to (18), there exists $\mu_2 > 0$ such that $\mathcal{B}_{\mu_2}(\mathbf{0}) \cap \mathcal{J}_0^\mathcal{W} = \emptyset$. Additionally, as per (21), there exists $\mu_3 > 0$ such that $\mathcal{B}_{\mu_3}(\mathbf{0}) \subset \mathcal{J}_1^\mathcal{W}$. We define the set $\mathcal{S}_\mu := \{\xi \in \mathcal{K} | \mathbf{x} \in \mathcal{B}_\mu(\mathbf{0})\}$, where $\mu \in (0, \min\{\mu_1, \mu_2, \mu_3\})$. Notice that for all initial conditions $\xi(0, 0) \in \mathcal{S}_\mu$, the control input, after at most one jump corresponds to the *move-to-target* mode and it steers the state \mathbf{x} towards the origin according to the control input vector $\mathbf{u}(\xi) = -\kappa_s \mathbf{x}, \kappa_s > 0$. Hence, for each $\mu \in (0, \min\{\mu_1, \mu_2, \mu_3\})$, the set \mathcal{S}_μ is forward invariant for the hybrid closed-loop system (31).

Consequently, for every $\rho > 0$, one can choose $\sigma \in (0, \min\{\mu_1, \mu_2, \mu_3, \rho\})$ such that for all initial conditions $\xi(0, 0)$ with $d(\xi(0, 0), \mathcal{A}) \leq \sigma$, one has $d(\xi(t, j), \mathcal{A}) \leq \rho$ for all $(t, j) \in \text{dom } \xi$, where $d(\xi, \mathcal{A})^2 = \inf_{(\mathbf{0}, \bar{\mathbf{h}}, \bar{\mathbf{a}}, \bar{m}, \bar{s}) \in \mathcal{A}} (\|\mathbf{x}\|^2 + \|\mathbf{h} - \bar{\mathbf{h}}\|^2 + \|\mathbf{a} - \bar{\mathbf{a}}\|^2 + (m - \bar{m})^2 + (s - \bar{s})^2) = \|\mathbf{x}\|^2$. Hence, according to [22, Definition 3.1], the target set \mathcal{A} is stable for the hybrid closed-loop system (31). Next, we proceed to establish the convergence properties of the set \mathcal{A} .

Attractivity: We aim to show that for the proposed hybrid closed-loop system (31), the target set \mathcal{A} is globally attractive in the set \mathcal{K} using [22, Definition 3.1 and Remark 3.5]. In other words, we prove that for all initial conditions $\xi(0, 0) \in \mathcal{F} \cup \mathcal{J} = \mathcal{K}$, every maximal solution ξ to the hybrid closed-loop system is complete and satisfies

$$\lim_{(t, j) \in \text{dom } \xi, t+j \rightarrow \infty} d(\xi(t, j), \mathcal{A}) = \|\mathbf{x}(t, j)\| = 0. \quad (36)$$

The completeness of all maximal solutions to the hybrid closed-loop system (31) follows from Lemma 3. Next, we

prove that for all initial condition $\xi(0,0) \in \mathcal{K}$, every complete solution ξ to the hybrid closed-loop system (31), satisfies (36). We consider two cases based on the initial value of the mode indicator variable $m(0,0)$.

Case 1: $m(0,0) = 0$. For the hybrid closed-loop system (31), consider a solution ξ initialized in the *move-to-target* mode. Let us assume $\xi(t_0, j_0) \in \mathcal{F}_0$ for some $(t_0, j_0) \in \text{dom } \xi$, $(t_0, j_0) \succeq (0,0)$. If $\xi(t, j) \notin \mathcal{J}_0$, for all $(t, j) \succeq (t_0, j_0)$, then the control input $\mathbf{u}(\mathbf{x}, \mathbf{h}, \mathbf{a}, 0, s) = -\kappa_s \mathbf{x}$ will steer the state \mathbf{x} straight towards the origin, where $\kappa_s > 0$. On the other hand, assume that there exists $(t_1, j_1) \succeq (t_0, j_0)$ such that $\xi(t_1, j_1) \in \mathcal{J}_0$. Then, according to (27), the control law switches to the *obstacle-avoidance* mode. As per (18), it is clear that $\mathbf{x}(t_1, j_1) \in \mathcal{J}_0^{\mathcal{W}} \cap \mathcal{N}_{\gamma_s}(\mathcal{D}_{r_a}(\mathcal{O}_i))$, for some $i \in \mathbb{I}$ and $d(\mathbf{x}(t_1, j_1), \mathcal{O}_i) = \beta$ for some $\beta \in [r_a, r_a + \gamma_s]$. At this instance, according to (27), the proposed navigation algorithm updates the values of the state variable $\mathbf{h}(t_1, j_1 + 1) = \mathbf{x}(t_1, j_1)$, $\mathbf{a}(t_1, j_1 + 1) \in \mathbf{A}(\mathbf{x}(t_1, j_1))$, $m(t_1, j_1 + 1) = 1$ and $s(t_1, j_1 + 1) = s(t_1, j_1) + 1$. According to (31), $\mathbf{h}(t_1, j_1 + 1) = \mathbf{h}(t, j)$, $\mathbf{a}(t_1, j_1 + 1) = \mathbf{a}(t, j)$ and $m(t_1, j_1 + 1) = m(t, j)$ for all $(t, j) \in (I_{j_1+1} \times j_1 + 1)$, where $I_{j_1+1} = \{t | (t, j_1 + 1) \in \text{dom } \xi\}$. To proceed with the proof, we need the following lemma:

Lemma 4. Under Assumption 1, consider a solution ξ to the hybrid closed-loop system (31). If $\xi(t_1, j_1) \in \mathcal{J}_0$ at some $(t_1, j_1) \in \text{dom } \xi$ such that $\mathbf{x}(t_1, j_1) \in \mathcal{J}_0^{\mathcal{W}} \cap \mathcal{N}_{\gamma}(\mathcal{D}_{r_a}(\mathcal{O}_i))$ for some $i \in \mathbb{I}$, then for all $(t, j) \in (I_{j_1+1} \times j_1 + 1)$, the following statements hold true:

- 1) $\mathbf{x}(t, j) \in \mathcal{P}(\mathbf{h}, \mathbf{a}) \cap \mathcal{N}_{\gamma}(\mathcal{D}_{r_a}(\mathcal{O}_i))$,
- 2) there exists $t_2 > t_1$ such that $t_2 < \infty$ and $\xi(t_2, j_1 + 1) \in \mathcal{J}_1$,

where $\mathbf{h} = \mathbf{h}(t_1, j_1 + 1) = \mathbf{h}(t, j)$ and $\mathbf{a} = \mathbf{a}(t_1, j_1 + 1) = \mathbf{a}(t, j)$.

Proof. See Appendix IX-E. \square

According to Lemma 4, when a solution ξ to the hybrid closed-loop system (31) evolves in the *obstacle-avoidance* mode, the state ξ eventually enters in the jump set of the *obstacle-avoidance* mode \mathcal{J}_1 (24) and the control law switches to the *move-to-target* mode.

According to Lemma 4, there exists $(t_2, j_1 + 1) \succ (t_1, j_1 + 1)$ with $t_2 < \infty$ such that $\xi(t_2, j_1 + 1) \in \mathcal{J}_1$. Notice that, according to (21) and (22), one has $\|\mathbf{x}(t_2, j_1 + 1)\| < \|\mathbf{x}(t_1, j_1 + 1)\|$. In other words, according to Lemma 4, the proposed navigation algorithm ensures that, at the instance where the control switches from the *obstacle-avoidance* mode to the *move-to-target* mode, the origin is closer to the point \mathbf{x} than to the last point where the control switched to the *obstacle-avoidance* mode. Furthermore, when the control input corresponds to the *move-to-target* mode, it steers the state \mathbf{x} towards the origin under the influence of control $\mathbf{u}(\xi) = -\kappa_s \mathbf{x}$, $\kappa_s > 0$. Consequently, given that the workspace \mathcal{W} and the obstacles $\mathcal{O}_i, i \in \mathbb{I} \setminus \{0\}$, are compact, it can be concluded that the solution $\xi(t, j)$ will contain finite number of jumps and will satisfy (36).

Case 2: $m(0,0) = 1$. For the hybrid closed-loop system (31) consider a solution ξ initialized in the *obstacle-avoidance*

mode. Since $m(0,0) = 1$, according to (24), $\xi(0,0) \in \mathcal{J}_1$. Therefore, according to (30), the control input switches to the *move-to-target* mode and $m(0,1) = 0$. One can now use arguments similar to the ones used for case 1 to show that the solution $\xi(t, j)$ will contain finite number of jumps and will satisfy (36).

Hence, the target set \mathcal{A} is globally attractive in the set \mathcal{K} for the proposed hybrid closed-loop system (31). In addition, since the set \mathcal{A} is stable for the hybrid closed-loop system (31), it is globally asymptotically stable in the set \mathcal{K} for the hybrid closed-loop system (31) as per [22, Remark 3.5].

E. Proof of Lemma 4

First, we prove that when the control input corresponds to the *obstacle-avoidance* mode, one has $\mathbf{x}(t, j) \in \mathcal{N}_{\gamma}(\mathcal{D}_{r_a}(\mathcal{O}_i))$ for all $(t, j) \in (I_{j_1+1}, j_1 + 1)$. To that end, we make use of Nagumo's theorem [11, Theorem 4.7] and show that when the control input corresponds to the *obstacle-avoidance* mode, one has

$$\mathbf{u}(\xi) \in \mathbf{T}_{\mathcal{N}_{\gamma}(\mathcal{D}_{r_a}(\mathcal{O}_i))}(\mathbf{x}), \quad (37)$$

for all $\mathbf{x} \in \partial \mathcal{N}_{\gamma}(\mathcal{D}_{r_a}(\mathcal{O}_i))$. This, combined with the fact that the control input vector $\mathbf{u}(\xi)$ is continuous, when it corresponds to the *obstacle-avoidance* mode, as stated in Lemma 2, ensures that $\mathbf{x}(t, j) \in \mathcal{N}_{\gamma}(\mathcal{D}_{r_a}(\mathcal{O}_i))$ for all $(t, j) \in (I_{j_1+1} \times j_1 + 1)$.

Note that $\partial \mathcal{N}_{\gamma}(\mathcal{D}_{r_a}(\mathcal{O}_i)) = \partial \mathcal{D}_{r_a}(\mathcal{O}_i) \cup \partial \mathcal{D}_{r_a+\gamma}(\mathcal{O}_i)$. For all $\mathbf{x} \in \partial \mathcal{D}_{r_a}(\mathcal{O}_i)$, one has $\mathcal{P}_{\geq}(\mathbf{0}, \mathbf{x}_{\pi}) \subset \mathbf{T}_{\mathcal{N}_{\gamma}(\mathcal{D}_{r_a}(\mathcal{O}_i))}(\mathbf{x})$, where $\mathbf{x}_{\pi} = \mathbf{x} - \Pi(\mathbf{x}, \mathcal{O}_{\mathcal{W}})$ with $\Pi(\mathbf{x}, \mathcal{O}_{\mathcal{W}}) = \Pi(\mathbf{x}, \mathcal{O}_i)$. Also, since the control input corresponds to the *obstacle-avoidance* mode, for $\mathbf{x} \in \partial \mathcal{D}_{r_a}(\mathcal{O}_i)$, the control vector (11a) is given by $\mathbf{u}(\xi) = \kappa_r \mathbf{P}(\mathbf{a}) \mathbf{x}_{\pi}$. Since for any $\mathbf{q} \in \mathbb{S}^2$, the matrix $\mathbf{P}(\mathbf{q})$ is positive semidefinite, one has $\mathbf{p}^{\top} \mathbf{P}(\mathbf{q}) \mathbf{p} \geq 0$ for all $\mathbf{p} \in \mathbb{R}^3$. Therefore, for all $\mathbf{x} \in \partial \mathcal{D}_{r_a}(\mathcal{O}_i)$, it is true that $\mathbf{x}_{\pi}^{\top} \mathbf{P}(\mathbf{a}) \mathbf{x}_{\pi} \geq 0$. This implies that $\mathbf{u}(\xi) \in \mathcal{P}_{\geq}(\mathbf{0}, \mathbf{x}_{\pi}) \subset \mathbf{T}_{\mathcal{N}_{\gamma}(\mathcal{D}_{r_a}(\mathcal{O}_i))}(\mathbf{x})$ for $\mathbf{x} \in \partial \mathcal{D}_{r_a}(\mathcal{O}_i)$, and condition (37) holds true.

Next, for $\mathbf{x} \in \partial \mathcal{D}_{r_a+\gamma}(\mathcal{O}_i)$, one has $\mathcal{P}_{\leq}(\mathbf{0}, \mathbf{x}_{\pi}) \subset \mathbf{T}_{\mathcal{N}_{\gamma}(\mathcal{D}_{r_a}(\mathcal{O}_i))}(\mathbf{x})$. Also, since the control input corresponds to the *obstacle-avoidance* mode, for $\mathbf{x} \in \partial \mathcal{D}_{r_a+\gamma}(\mathcal{O}_i)$, the control vector (11a) is given by $\mathbf{u}(\xi) = -\kappa_r \mathbf{P}(\mathbf{a}) \mathbf{x}_{\pi}$. As mentioned earlier, for all $\mathbf{x} \in \partial \mathcal{D}_{r_a+\gamma}(\mathcal{O}_i)$, one has $\mathbf{x}_{\pi}^{\top} \mathbf{P}(\mathbf{a}) \mathbf{x}_{\pi} \geq 0$. Therefore, $\mathbf{u}(\xi) \in \mathcal{P}_{\leq}(\mathbf{0}, \mathbf{x}_{\pi}) \subset \mathbf{T}_{\mathcal{N}_{\gamma}(\mathcal{D}_{r_a}(\mathcal{O}_i))}(\mathbf{x})$ for $\mathbf{x} \in \partial \mathcal{D}_{r_a+\gamma}(\mathcal{O}_i)$, and condition (37) holds true. As a result, since $\mathbf{x}(t_1, j_1 + 1) \in \mathcal{N}_{\gamma}(\mathcal{D}_{r_a}(\mathcal{O}_i))$, one can conclude that

$$\mathbf{x}(t, j) \in \mathcal{N}_{\gamma}(\mathcal{D}_{r_a}(\mathcal{O}_i)), \quad (38)$$

for all $(t, j) \in (I_{j_1+1}, j_1 + 1)$.

Next, we show that when the control input corresponds to the *obstacle-avoidance* mode, $\mathbf{x}(t, j) \in \mathcal{N}_{\gamma}(\mathcal{D}_{r_a}(\mathcal{O}_i)) \cap \mathcal{P}(\mathbf{h}, \mathbf{a})$ for all $(t, j) \in (I_{j_1+1}, j_1 + 1)$. When the control input corresponds to the *obstacle-avoidance* mode, it is given by $\mathbf{u}(\xi) = \kappa_r \mathbf{v}(\mathbf{x}, \mathbf{a})$, which, as per (12), can be expressed as a linear combination of the vectors $\mathbf{P}(\mathbf{a}) \mathbf{x}_{\pi}$ and $\mathbf{R}(\mathbf{a}) \mathbf{P}(\mathbf{a}) \mathbf{x}_{\pi}$. Since $\mathbf{P}(\mathbf{a})$, defined in (13), is an orthogonal projection operator and $\mathbf{0} \in \mathcal{P}(\mathbf{h}, \mathbf{a})$, for all $\mathbf{x} \in \mathcal{N}_{\gamma}(\mathcal{D}_{r_a}(\mathcal{O}_i)) \cap \mathcal{P}(\mathbf{h}, \mathbf{a})$, one has $\mathbf{P}(\mathbf{a}) \mathbf{x}_{\pi} \in \mathcal{P}(\mathbf{h}, \mathbf{a})$. Additionally, one can show that $\mathbf{R}(\mathbf{a}) \mathbf{P}(\mathbf{a}) \mathbf{x}_{\pi} \in \mathcal{P}(\mathbf{h}, \mathbf{a})$. Therefore, for all $\mathbf{x} \in \mathcal{N}_{\gamma}(\mathcal{D}_{r_a}(\mathcal{O}_i)) \cap \mathcal{P}(\mathbf{h}, \mathbf{a})$, one has $\mathbf{v}(\mathbf{x}, \mathbf{a}) \in \mathcal{P}(\mathbf{h}, \mathbf{a})$. As a

result, since $\mathbf{x}(t_1, j_1 + 1) \in \mathcal{N}_\gamma(\mathcal{D}_{r_a}(\mathcal{O}_i)) \cap \mathcal{P}(\mathbf{h}, \mathbf{a})$, using (38), one can conclude that

$$\mathbf{x}(t, j) \in \mathcal{N}_\gamma(\mathcal{D}_{r_a}(\mathcal{O}_i)) \cap \mathcal{P}(\mathbf{h}, \mathbf{a}),$$

for all $(t, j) \in (I_{j_1+1}, j_1 + 1)$ and claim 1 in Lemma 4 is satisfied.

Next, we proceed to prove claim 2 in Lemma 4 which states that when $\xi(t_1, j_1 + 1) \in \mathcal{F}_1$ for some $(t_1, j_1 + 1) \in \text{dom } \xi$, the control input steers the state ξ to the jump set \mathcal{J}_1 of the *obstacle-avoidance* mode in finite time $(t_2, j_1 + 1) \succ (t_1, j_1 + 1)$ with $t_2 < \infty$.

Let us define the set $\mathcal{O}_i^S = \mathcal{D}_{r_a}(\mathcal{O}_i) \cap \mathcal{P}(\mathbf{h}, \mathbf{a})$, as shown in Fig. 3. Since obstacle \mathcal{O}_i is convex, the set \mathcal{O}_i^S is also convex. As a result, the target location has a unique closest point on the set \mathcal{O}_i^S , represented by $\Pi(\mathbf{0}, \mathcal{O}_i^S)$. We define a set \mathcal{LS} as follows:

$$\mathcal{LS} := \mathcal{L}(\mathbf{0}, \mathbf{0}_\pi^S) \cap \mathcal{N}_\gamma(\mathcal{D}_{r_a}(\mathcal{O}_i)) \cap \mathcal{P}_{\geq}(\mathbf{0}_\pi^S, -\mathbf{0}_\pi^S), \quad (39)$$

where $\mathbf{0}_\pi^S = \Pi(\mathbf{0}, \mathcal{O}_i^S)$. Since $\mathbf{0} \in \mathcal{P}(\mathbf{h}, \mathbf{a})$ and $\mathcal{O}_i^S \subset \mathcal{P}(\mathbf{h}, \mathbf{a})$, the line segment \mathcal{LS} belongs to the plane $\mathcal{P}(\mathbf{h}, \mathbf{a})$. Since $\mathcal{LS} \cap \mathcal{D}_{r_a}^\circ(\mathcal{O}_i) = \emptyset$, the line segment \mathcal{LS} also belongs to the *exit* region \mathcal{R}_e (17). Since the *hit point* \mathbf{h} belongs to \mathcal{R}_i^l , the target location $\mathbf{0}$ is closer to $\Pi(\mathbf{0}, \mathcal{O}_i^S)$ than to \mathbf{h} . Hence, if $\mathbf{0} \notin \mathcal{D}_{r_a+\gamma}(\mathcal{O}_i)$, then for a sufficiently small value of $\bar{\epsilon}$, used in (22), one can ensure that the set \mathcal{LS} belongs to the set \mathcal{J}_1^W (21). On the other hand, if $\mathbf{0} \in \mathcal{N}_\gamma(\mathcal{D}_{r_a}(\mathcal{O}_i))$, it is straightforward to verify that $\mathcal{LS} \subset \mathcal{S}_0$, which, according to (21), implies that $\mathcal{LS} \subset \mathcal{J}_1^W$.

Now, if one ensures that the state \mathbf{x} , which belongs to the set $\mathcal{N}_\gamma(\mathcal{D}_{r_a}(\mathcal{O}_i)) \cap \mathcal{P}(\mathbf{h}, \mathbf{a})$ after time (t_1, j_1) , in the *obstacle-avoidance* mode around obstacle \mathcal{O}_i , eventually intersects the set \mathcal{LS} at some finite time $(t_2, j_1 + 1) \succ (t_1, j_1 + 1)$, then it will imply that $\xi(t_2, j_1 + 1) \in \mathcal{J}_1$, and claim 2 in Lemma 4 will be proven. To that end, let us divide the set $\mathcal{N}_\gamma(\mathcal{D}_{r_a}(\mathcal{O}_i)) \cap \mathcal{P}(\mathbf{h}, \mathbf{a})$, as shown in Fig. 3, into 3 separate subsets as follows:

$$\mathcal{N}_\gamma(\mathcal{D}_{r_a}(\mathcal{O}_i)) \cap \mathcal{P}(\mathbf{h}, \mathbf{a}) = \mathcal{S}_1 \cup \mathcal{S}_2 \cup \mathcal{S}_3, \quad (40)$$

where the sets $\mathcal{S}_1, \mathcal{S}_2$ and \mathcal{S}_3 are defined as follows:

$$\begin{aligned} \mathcal{S}_1 &= \mathcal{N}_{\gamma_a}(\mathcal{D}_{r_a}(\mathcal{O}_i)) \cap \mathcal{P}(\mathbf{h}, \mathbf{a}), \\ \mathcal{S}_2 &= \mathcal{N}_{\gamma_s-\gamma_a}^\circ(\mathcal{D}_{r_a+\gamma_a}(\mathcal{O}_i)) \cap \mathcal{P}(\mathbf{h}, \mathbf{a}), \\ \mathcal{S}_3 &= \mathcal{N}_{\gamma-\gamma_s}(\mathcal{D}_{r_a+\gamma_s}(\mathcal{O}_i)) \cap \mathcal{P}(\mathbf{h}, \mathbf{a}), \end{aligned} \quad (41)$$

where $0 < \gamma_a < \gamma_s < \gamma$.

We show that when the control input corresponds to the *obstacle-avoidance* mode and the state \mathbf{x} belongs either in the set \mathcal{S}_1 or in the set \mathcal{S}_3 , the control eventually steers the state \mathbf{x} to the set \mathcal{S}_2 . Then, we show that for all $\mathbf{x} \in \mathcal{S}_2$, the control vector $\mathbf{u}(\xi)$ belongs to the open positive half-space $\mathcal{P}_{>}(\mathbf{0}, \mathbf{R}(\mathbf{a})\mathbf{P}(\mathbf{a})\mathbf{x}_\pi)$. This implies that the state \mathbf{x} , which belongs to the set $\mathcal{N}_\gamma(\mathcal{D}_{r_a}(\mathcal{O}_i)) \cap \mathcal{P}(\mathbf{h}, \mathbf{a})$ after time (t_1, j_1) , in the *obstacle-avoidance* mode around obstacle \mathcal{O}_i , is always steered to the open positive half-space $\mathcal{P}_{>}(\mathbf{0}, \mathbf{R}(\mathbf{a})\mathbf{P}(\mathbf{a})\mathbf{x}_\pi)$ and will eventually reach the set \mathcal{LS} at some finite time $(t_2, j_1 + 1) \succ (t_1, j_1 + 1)$.

First, we show that when the control input corresponds to the *obstacle-avoidance* mode and the state \mathbf{x} is either in the set \mathcal{S}_1 or in the set \mathcal{S}_3 , the control will eventually steer the

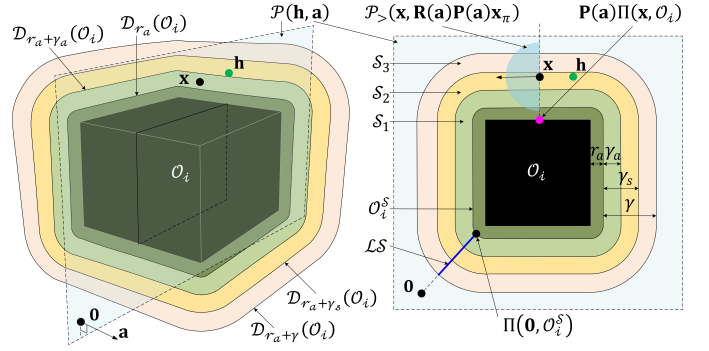


Fig. 3: The partition of the set $\mathcal{N}_\gamma(\mathcal{D}_{r_a}(\mathcal{O}_i)) \cap \mathcal{P}(\mathbf{h}, \mathbf{a})$.

state \mathbf{x} to the set \mathcal{S}_2 .

When the control input corresponds to the *obstacle-avoidance* mode and \mathbf{x} belongs to the set \mathcal{S}_1 , the control vector $\mathbf{u}(\xi)$ in (11a) becomes

$$\mathbf{u}(\xi) = \kappa_r \mathbf{P}(\mathbf{a})\mathbf{x}_\pi, \kappa_r > 0. \quad (42)$$

Let $\mathbf{x} \in \partial \mathcal{D}_{r_a+\beta}(\mathcal{O}_i) \cap \mathcal{S}_1$ for some $\beta \in [0, \gamma_a]$. We know that for $\mathbf{x} \in \partial \mathcal{D}_{r_a+\beta}(\mathcal{O}_i) \cap \mathcal{S}_1$, the tangent cone to the set $\mathcal{N}_{\gamma-\beta}(\mathcal{D}_{r_a+\beta}(\mathcal{O}_i))$ at \mathbf{x} is given by

$$\mathbf{T}_{\mathcal{N}_{\gamma-\beta}(\mathcal{D}_{r_a+\beta}(\mathcal{O}_i))}(\mathbf{x}) = \mathcal{P}_{\geq}(\mathbf{0}, \mathbf{x}_\pi).$$

If we show that for all $\mathbf{x} \in \partial \mathcal{D}_{r_a+\beta}(\mathcal{O}_i) \cap \mathcal{S}_1$, one has $\mathbf{x}_\pi^\top \mathbf{P}(\mathbf{a})\mathbf{x}_\pi > 0$, then it implies that the control input vector (42) steers \mathbf{x} to the interior of the set $\mathcal{N}_{\gamma-\beta}(\mathcal{D}_{r_a+\beta}(\mathcal{O}_i))$. This, combined with the fact that $\mathbf{x}(t, j) \in \mathcal{P}(\mathbf{h}, \mathbf{a})$, for all $(t, j) \in (I_{j_1+1} \times j_1 + 1)$, as per claim 1 in Lemma 4, ensures that the control input vector (42) steers \mathbf{x} to the interior of the set $(\mathcal{S}_1 \cup \mathcal{S}_2) \setminus \mathcal{D}_{r_a+\beta}^\circ(\mathcal{O}_i)$ and eventually \mathbf{x} will enter in the set \mathcal{S}_2 . To proceed with the proof we require the following fact:

Fact 1: Let us consider the hyperplane $\mathcal{P}(\mathbf{p}, \mathbf{q})$, where $\mathbf{p} \in \mathcal{J}_0^W \cap \mathcal{N}_\gamma(\mathcal{D}_{r_a}(\mathcal{O}_i))$, for some $i \in \mathbb{I}$ and $\mathbf{q} \in \mathbf{A}(\mathbf{p})$, where the mapping \mathbf{A} is defined in (28). Then, for all $\mathbf{x} \in \mathcal{N}_\gamma(\mathcal{D}_{r_a}(\mathcal{O}_i)) \cap \mathcal{P}(\mathbf{p}, \mathbf{q})$, one has $\mathbf{x}_\pi^\top \mathbf{P}(\mathbf{q})\mathbf{x}_\pi > 0$.

Proof. This proof is by contradiction. First, note that for any $\mathbf{q} \in \mathbb{S}^2$, the matrix $\mathbf{P}(\mathbf{q})$ is positive semidefinite. Therefore, for any vector $\mathbf{s} \in \mathbb{R}^n$, one has $\mathbf{s}^\top \mathbf{P}(\mathbf{q})\mathbf{s} \geq 0$. Let us assume that there exists $\mathbf{x} \in \mathcal{N}_\gamma(\mathcal{D}_{r_a}(\mathcal{O}_i)) \cap \mathcal{P}(\mathbf{p}, \mathbf{q})$ such that $\mathbf{x}_\pi^\top \mathbf{P}(\mathbf{q})\mathbf{x}_\pi = 0$. Since $\mathbf{x}_\pi \neq \mathbf{0}$, one has $\mathbf{P}(\mathbf{q})\mathbf{x}_\pi = \mathbf{0}$. Therefore, the vector \mathbf{x}_π is normal to the hyperplane $\mathcal{P}(\mathbf{p}, \mathbf{q})$. This implies that the plane $\mathcal{P}(\mathbf{p}, \mathbf{q})$ is a supporting hyperplane [23, Section 2.5.2] to the convex set $\mathcal{D}_{r_a+\beta}(\mathcal{O}_i)$ at \mathbf{x} , where $\beta = d(\mathbf{x}, \mathcal{O}_i) - r_a \in [0, \gamma]$. Therefore, the set $\mathcal{D}_{r_a}^\circ(\mathcal{O}_i) \cap \mathcal{P}(\mathbf{p}, \mathbf{q})$ is an empty set.

However, since $\mathbf{q} \in \mathbf{A}(\mathbf{p})$, according to (28), one has $\mathbf{p}_\pi \in \mathcal{P}(\mathbf{p}, \mathbf{q})$ and $\mathbf{0} \in \mathcal{P}(\mathbf{p}, \mathbf{q})$. Therefore, $\mathcal{L}(\mathbf{p}, \Pi(\mathbf{p}, \mathcal{O}_i)) \subset \mathcal{P}(\mathbf{p}, \mathbf{q})$. As a result, $\mathcal{L}(\mathbf{p}, \Pi(\mathbf{p}, \mathcal{O}_i)) \cap \mathcal{D}_{r_a}^\circ(\mathcal{O}_i) \neq \emptyset$. This implies that $\mathcal{D}_{r_a}^\circ(\mathcal{O}_i) \cap \mathcal{P}(\mathbf{p}, \mathbf{q}) \neq \emptyset$, which is a contradiction. \square

According to Fact 1, for all $\mathbf{x} \in \partial \mathcal{D}_{r_a+\beta}(\mathcal{O}_i) \cap \mathcal{S}_1$, where $\beta \in [0, \gamma_a]$, one has $\mathbf{x}_\pi^\top \mathbf{P}(\mathbf{a})\mathbf{x}_\pi > 0$. Therefore, as discussed earlier, the control input vector (42) steers \mathbf{x} to the interior of

the set $(\mathcal{S}_1 \cup \mathcal{S}_2) \setminus \mathcal{D}_{r_a+\beta}^\circ(\mathcal{O}_i)$ and eventually \mathbf{x} will enter in the set \mathcal{S}_2 .

Similarly, when the control input corresponds to the *obstacle-avoidance* mode and \mathbf{x} belongs to the set \mathcal{S}_3 , the control vector $\mathbf{u}(\xi)$ in (11a) is given by

$$\mathbf{u}(\xi) = -\kappa_r \mathbf{P}(\mathbf{a})\mathbf{x}_\pi, \kappa_r > 0. \quad (43)$$

Let $\mathbf{x} \in \partial\mathcal{D}_{r_a+\beta}(\mathcal{O}_i) \cap \mathcal{S}_3$ for some $\beta \in [\gamma_s, \gamma]$. We know that for $\mathbf{x} \in \partial\mathcal{D}_{r_a+\beta}(\mathcal{O}_i) \cap \mathcal{S}_3$, the tangent cone to the set $\mathcal{D}_{r_a+\beta}(\mathcal{O}_i)$ at \mathbf{x} is given by

$$\mathbf{T}_{\mathcal{D}_{r_a+\beta}(\mathcal{O}_i)}(\mathbf{x}) = \mathcal{P}_{\leq}(\mathbf{0}, \mathbf{x}_\pi).$$

According to Fact 1, for all $\mathbf{x} \in \partial\mathcal{D}_{r_a+\beta}(\mathcal{O}_i) \cap \mathcal{S}_3$, where $\beta \in [\gamma_s, \gamma]$, one has $\mathbf{x}_\pi^\top \mathbf{P}(\mathbf{a})\mathbf{x}_\pi > 0$. This implies that the control input vector (43) steers \mathbf{x} to the interior of the set $\mathcal{D}_{r_a+\beta}(\mathcal{O}_i)$. This, combined with the fact that $\mathbf{x}(t, j) \in \mathcal{P}(\mathbf{h}, \mathbf{a})$, for all $(t, j) \in (I_{j_1+1} \times j_1 + 1)$, as per claim 1 in Lemma 4, ensures that the control input vector (43) steers \mathbf{x} to the interior of the set $(\mathcal{S}_3 \cup \mathcal{S}_2) \cap \mathcal{D}_{r_a+\beta}^\circ(\mathcal{O}_i)$ and eventually \mathbf{x} will enter in the set \mathcal{S}_2 .

Finally, we show that when the control input corresponds to the *obstacle-avoidance* mode and the state \mathbf{x} belongs to the set \mathcal{S}_2 , the control vector $\mathbf{u}(\xi)$ belongs to the open positive half-space $\mathcal{P}_{>}(\mathbf{0}, \mathbf{R}(\mathbf{a})\mathbf{P}(\mathbf{a})\mathbf{x}_\pi)$. When the control law operates in the *obstacle-avoidance* mode and the state $\mathbf{x} \in \mathcal{S}_2$, according to (11), one has $\mathbf{u}(\xi) = \kappa_r \mathbf{v}(\mathbf{x}, \mathbf{a}), \kappa_r > 0$. Note that for all $\mathbf{x} \in \mathcal{S}_2$, one has $\eta(\mathbf{x}) \in (-1, 1)$. Therefore, for every $\mathbf{x} \in \mathcal{S}_2$, the vector $\mathbf{v}(\mathbf{x}, \mathbf{a})$ can be expressed as a linear combination of the vectors $\mathbf{P}(\mathbf{a})\mathbf{x}_\pi$ and $\mathbf{R}(\mathbf{a})\mathbf{P}(\mathbf{a})\mathbf{x}_\pi$ given by

$$\mathbf{v}(\mathbf{x}, \mathbf{a}) = k_1 \mathbf{P}(\mathbf{a})\mathbf{x}_\pi + k_2 \mathbf{R}(\mathbf{a})\mathbf{P}(\mathbf{a})\mathbf{x}_\pi, \quad (44)$$

where $k_1 \in \mathbb{R}$ and $k_2 > 0$. Additionally, according to Fact 1, for all $\mathbf{x} \in \mathcal{S}_2$, one has $\mathbf{P}(\mathbf{a})\mathbf{x}_\pi \neq \mathbf{0}$. As a result, it can be confirmed that $\mathbf{v}(\mathbf{x}, \mathbf{a})^\top \mathbf{R}(\mathbf{a})\mathbf{P}(\mathbf{a})\mathbf{x}_\pi > 0$, when the state \mathbf{x} belongs to the set \mathcal{S}_2 , and the proof is complete.

REFERENCES

- [1] D. Koditschek and E. Rimon, "Exact robot navigation using artificial potential functions," *IEEE Trans. Robot. Automat.*, vol. 8, pp. 501–518, 1992.
- [2] C. Li and H. G. Tanner, "Navigation functions with time-varying destination manifolds in star worlds," *IEEE Transactions on Robotics*, vol. 35, no. 1, pp. 35–48, 2018.
- [3] S. Paternain, D. E. Koditschek, and A. Ribeiro, "Navigation functions for convex potentials in a space with convex obstacles," *IEEE Transactions on Automatic Control*, vol. 63, no. 9, pp. 2944–2959, 2017.
- [4] H. Kumar, S. Paternain, and A. Ribeiro, "Navigation of a quadratic potential with ellipsoidal obstacles," *Automatica*, vol. 146, p. 110643, 2022.
- [5] A. D. Ames, X. Xu, J. W. Grizzle, and P. Tabuada, "Control barrier function based quadratic programs for safety critical systems," *IEEE Transactions on Automatic Control*, vol. 62, no. 8, pp. 3861–3876, 2016.
- [6] L. Wang, A. D. Ames, and M. Egerstedt, "Safety barrier certificates for collisions-free multirobot systems," *IEEE Transactions on Robotics*, vol. 33, no. 3, pp. 661–674, 2017.
- [7] A. Singletary, K. Klingebiel, J. Bourne, A. Browning, P. Tokumaru, and A. Ames, "Comparative analysis of control barrier functions and artificial potential fields for obstacle avoidance," in *2021 IEEE/RSJ International Conference on Intelligent Robots and Systems (IROS)*. IEEE, 2021, pp. 8129–8136.
- [8] M. F. Reis, A. P. Aguiar, and P. Tabuada, "Control barrier function-based quadratic programs introduce undesirable asymptotically stable equilibria," *IEEE Control Systems Letters*, vol. 5, no. 2, pp. 731–736, 2020.
- [9] X. Tan and D. V. Dimarogonas, "On the undesired equilibria induced by control barrier function based quadratic programs," *Automatica*, vol. 159, p. 111359, 2024.
- [10] L. Smaili and S. Berkane, "Real-time sensor-based feedback control for obstacle avoidance in unknown environments," *arXiv preprint arXiv:2403.08614*, 2024.
- [11] F. Blanchini, S. Miani et al., *Set-theoretic methods in control*. Springer, 2008, vol. 78.
- [12] O. Arslan and D. E. Koditschek, "Sensor-based reactive navigation in unknown convex sphere worlds," *The International Journal of Robotics Research*, vol. 38, no. 2-3, pp. 196–223, 2019.
- [13] D. E. Koditschek and E. Rimon, "Robot navigation functions on manifolds with boundary," *Advances in applied mathematics*, vol. 11, no. 4, pp. 412–442, 1990.
- [14] S. G. Loizou, H. G. Tanner, V. Kumar, and K. J. Kyriakopoulos, "Closed loop motion planning and control for mobile robots in uncertain environments," in *IEEE Conference on Decision and Control*, vol. 3, 2003, pp. 2926–2931.
- [15] A. S. Matveev, H. Teimoori, and A. V. Savkin, "A method for guidance and control of an autonomous vehicle in problems of border patrolling and obstacle avoidance," *Automatica*, vol. 47, no. 3, pp. 515–524, 2011.
- [16] P. Braun, C. M. Kellett, and L. Zaccarian, "Explicit construction of stabilizing robust avoidance controllers for linear systems with drift," *IEEE Transactions on Automatic Control*, vol. 66, no. 2, pp. 595–610, 2020.
- [17] S. Berkane, A. Bisoffi, and D. V. Dimarogonas, "Obstacle avoidance via hybrid feedback," *IEEE Transactions on Automatic Control*, vol. 67, no. 1, pp. 512–519, 2021.
- [18] M. Sawant, S. Berkane, I. Polushin, and A. Tayebi, "Hybrid feedback for autonomous navigation in planar environments with convex obstacles," *IEEE Transactions on Automatic Control*, vol. 68, no. 12, pp. 7342–7357, 2023.
- [19] M. Sawant, I. Polushin, and A. Tayebi, "Hybrid feedback control design for non-convex obstacle avoidance," *IEEE Transactions on Automatic Control*, pp. 1–16, 2024, doi: 10.1109/TAC.2024.3388952.
- [20] R. Goebel, R. G. Sanfelice, and A. R. Teel, *Hybrid dynamical systems*. Princeton University Press, 2012.
- [21] J. Rataj and M. Zähle, *Curvature measures of singular sets*. Springer, 2019.
- [22] R. G. Sanfelice, *Hybrid feedback control*. Princeton University Press, 2021.
- [23] S. Boyd, S. P. Boyd, and L. Vandenberghe, *Convex optimization*. Cambridge university press, 2004.